MAUSAM, **75**, 1 (January 2024), 215-236

MAUSAM

DOI : https://doi.org/10.54302/mausam.v75i1.5960
Homepage: https://mausamjournal.imd.gov.in/index.php/MAUSAM

UDC No. 502 : 544.77 (540.65)

Seasonal characterization of aerosols over high altitude location of southern India, Ooty, Tamilnadu

R. M. JAYABALAKRISHNAN, G. SIVASANKARAN[#], M. MAHESWARI,

R. KUMARAPERUMAL* and C. POORNACHANDRA

Department of Environmental Sciences, TNAU, Coimbatore – 641 003, India

**Department of Remote sensing and Geographic Information System,*

TNAU, Coimbatore – 641 003, India

(*Received 11 May 2021, Accepted 14 March 2022*)

e mail : sivag26398@gmail.com

सार – एरोसोल से जलवायु परिवर्तन की स्थिति खराब हुई है जिससे जलवायु परिवर्तन की स्थितियों को समझने के लिए वैज्ञानिक अनुसंधान में महत्वपूर्ण स्थान मिला है। इसलिए, एरोसोल के ऑप्टिकल गुण पृथ्वी के ऊर्जा विकिरण बजट में महत्वपूर्ण भूमिका निभाते हैं। ऊटी में ऊंचाई वाले क्षेत्र में दिसंबर 2020 से मई 2021 तक एरोसोल ऑप्टिकल गहराई मापी गई। एओडी की वर्णक्रमीय, मासिक और दैनिक भिन्नता का आकलन किया गया और उनकी ऋतुनिष्ठ परिवर्तनशीलता दिखाई गई। 500 nm पर औसत AOD का मान शीत ऋतु (0.213±0.006) की तुलना में ग्रीष्मन ऋतु (0.625±0.323) के दौरान अधिक था। दिसंबर 2020 से सितंबर 2021 तक एथलोमीटर का उपयोग करकेकाला कार्बन (BC) को मापा गया। काला कार्बन की ऋतुवार औसत सांद्रताशीत, ग्रीष्म और मानसून ऋतु में क्रमशः 0.680±0.206 µg m^{-3}, 1.128±0.393 µg m^{-3} और 0.189±0.06 µg m^{-3} थी। काला कार्बन के द्रव्यमान सांद्रता के स्रोतों को जीवाश्म ईंधन (BCff) और बायोमास जलने (BCbb) के आधार पर विभाजित किया गया। कुल काला कार्बन सांद्रता में जीवाश्म ईंधन का योगदानबायोमास के योगदान से अधिक था। AOD के साथ कालाकार्बन की सांघ्रता की तुलनात्मक अध्ययन में यह अनुमान लगाया गया कि अप्रैल, 2021 तक काला कार्बन सांद्रता में वृद्धि के अनुरूप AOD में वृद्धि हुई थी। जमीन आधारित दैनिक AOD माप की तुलना MODIS द्वारा प्राप्त AOD के साथ की गई थी। MODIS द्वारा प्राप्त AOD को शीत और ग्रीष्म ऋतु के दौरान जमीन पर मापे गए AOD के साथ सकारात्मक रूप से सहसंबद्ध किया गया। HYSPLIT प्रक्षेपवक्र ने दीर्घ अवधि के क्षेत्रों से स्रोत के मार्ग प्रस्तुत किए। शीत ऋतु के प्रक्षेपवक्र का श्रेय उत्तर-पूर्वी और पूर्वी हवाओं को दिया गया और ग्रीष्म ऋतु को उत्तर-पश्चिमी और पश्चिमी हवाओं को जिम्मेदार ठहराया गया, जो पड़ोसी शहरों से एरोसोल के लंबी दूरी के परिवहन को प्रदर्शित करता है। मौसम संबंधी प्राचलों ने सभी ऋतुओं के दौरान एरोसोल की लोडिंग को महत्वपूर्ण रूप से प्रभावित किया, जो यह दर्शाता है कि वे स्थानीय प्रचलित मौसम संबंधी स्थितियों के अनुरूप थे।

ABSTRACT. Climate change has been worsened by aerosols which got a significant place in the scientific research to understand climate change dynamics. Hence, the optical properties of the aerosols play an important role in the earth's energy radiation budget. The Aerosol Optical Depth was measured at high altitude region in Ooty from December 2020 to May 2021. The spectral, monthly and diurnal variation of AOD were assessed and showed their seasonal variability. The mean AOD value at 500 nm was higher during the Summer season (0.625±0.323) than in the Winter season (0.213±0.006). The Black Carbon (BC) was measured using an Aethalo meter from December 2020 to September 2021. The average season wise concentrations of BC were 0.680±0.206µg m^{-3}, 1.128±0.393 µg m^{-3} and 0.189±0.06 µg m^{-3} for the Winter, Summer and Monsoon seasons, respectively. The sources of BC mass concentration were apportioned based on fossil fuel (BCff) and biomass burning (BCbb). The fossil fuel based contribution was higher than the biomass based contribution to the total BC concentration. The comparative study of BC concentration with the AOD, it was projected that the AOD had increased in line with surging BC concentration up to April, 2021. The ground-based daily AOD measurements were compared with the MODIS retrieved AOD. The MODIS retrieved AOD was positively correlated with the ground measured AOD during the Winter and Summer seasons. The HYSPLIT trajectory presented the pathways of the source from the long range regions. The Winter season trajectory was attributed to the North-easterly and easterly winds and the Summer season was attributed to the North-westerly and westerly winds that exhibited the long-range transport of aerosols from the neighbouring cities. The meteorological parameters significantly

affected the loading of aerosols during all the seasons, denoting that they were supposed to the local prevailing meteorological conditions.

Key words – AOD, Black Carbon, Source apportionment, MODIS, Meteorological parameters.

1. Introduction

Rapid growing population, urbanization bolstered byhuman economic development paves the way for air pollution the worldwide. Air pollution is caused by the emission of particulate matter, especially the anthropogenic aerosols that affect the earth's radiative properties and worsen the climatic patterns. Aerosol loading has been steadily growing in South and East Asia (mostly India and China) as a result of rapid urbanisation and rising population density along with rising energy demands (Tiwari *et al*., 2018). Aerosols in the atmosphere influence the climate in both direct and indirect ways. They have a direct effect because they scatter and absorb solar and terrestrial radiation. It is necessary to understand the optical properties of aerosols, as well as their spatial and temporal variability in order to comprehend their impact on climate (Taneja *et al*., 2017). Single scattering albedo (SSA), Aerosol Optical Depth (AOD), asymmetry factor (Assy), surface albedo, concentration of aerosols, composition, size and structure are some of the main parameters that determine the radiative effects of aerosol particles (Kumar *et al*., 2020). In this context, AOD spectral analysis provides useful information about the different types of aerosols, their sources and their climatic impacts (Dhar *et al*., 2018).

The Aerosol Optical Depth (AOD) is a critical measure that connects incoming solar radiation to aerosol properties like mass loading, size distribution and type (Singh *et al*., 2020). As per the observations, Aerosol optical depth (AOD) was found to be increasing at a rate of 2.3 per cent (of its value in 1985) per year on average and at a faster pace (4%) during the last decadeover eastern and southern Asia (Stocker *et al*., 2013). If current trends continue, AOD would nearly double and reach the same in several regions during the next several decades, resulting in a two-fold increase in aerosol-induced lower atmospheric warming (Krishna Moorthy *et al*., 2013). Carbonaceous aerosols (soot) are formed by the combustion of fossil fuels and biomass and they contain both Black Carbon (BC) and Organic Carbon (OC). BC is emitted as primary particles due to incomplete fuel combustion whereas, OC is emitted as both primary and secondary particles as a result of hydrocarbon condensation or gas-phase oxidation (Pavankumari, 2015). Black carbon (BC) was an anthropogenic aerosol which was second most contributor for the global warming next to the CO_2. The sources of BC are fossil fuel (FF) combustion and biomass burning (BB) (Resquin *et al*., 2018). According to a recent study, the annual BC emission rate in the Indian subcontinent is 388-1344 Gg yr^{-1} (Verma *et al*., 2017). The estimated global mean BC radiative force (0.64 Wm^{-2}) is supported by a large uncertainty of about 0.5 Wm^{-2} (Srivastava *et al*., 2021). BC has different optical and radiative properties than other aerosols as it is an absorbing part of carbonaceous aerosols (Singh *et al*., 2018).

India is also one of the major contributors to the emission of a wide variety of aerosols. In this concern, to gather a comprehensive view of the aerosol trends in India, ground-based aerosol monitoring observatories have been set up in various parts of India as part of the ISRO-GBP supported Aerosol Radiative Forcing over India (ARFI) project with currently operating 42 sites, which measures several aerosol characteristics (Singh *et al*., 2020).

The high-altitude site that we have chosen for the study lies more or less above the atmospheric boundary layer, thus, the prediction of climate anomalies will be easier. This exclusive pattern provides the scientific interest in studying the aerosol characteristics and their seasonal, temporal variations at this high-altitude location in the Nilgiris Biosphere.

2. Materials and methods

2.1. *Description of study site*

The study site was located near to Ooty town, the part of the Western Ghats of Southern India. Ooty, an important tourist spot in Southern India and known for its peculiar weather conditions, is attributed to dense forest and a wide range of biodiversity, making it an important biosphere area of the Tamilnadu state. The Study site, ISRO-ARFI observatory was located (Latitude - 11° 25'27" N, Longitude - 76°43'27" E) at the altitude of 2520 m amsl (Fig. 1), which was subdued by anthropogenic activities and known as clean site, which is 7 km away from the Ooty town. The entire study has been conducted at the premises of ISRO-ARFI Observatory.

2.2. *General meteorological description of the study site*

The study period from December, 2020 to September, 2021 were categorized as following the criteria given by the Indian Meteorological Department (IMD) and with the consideration of local meteorological conditions, with this concern, the seasons were

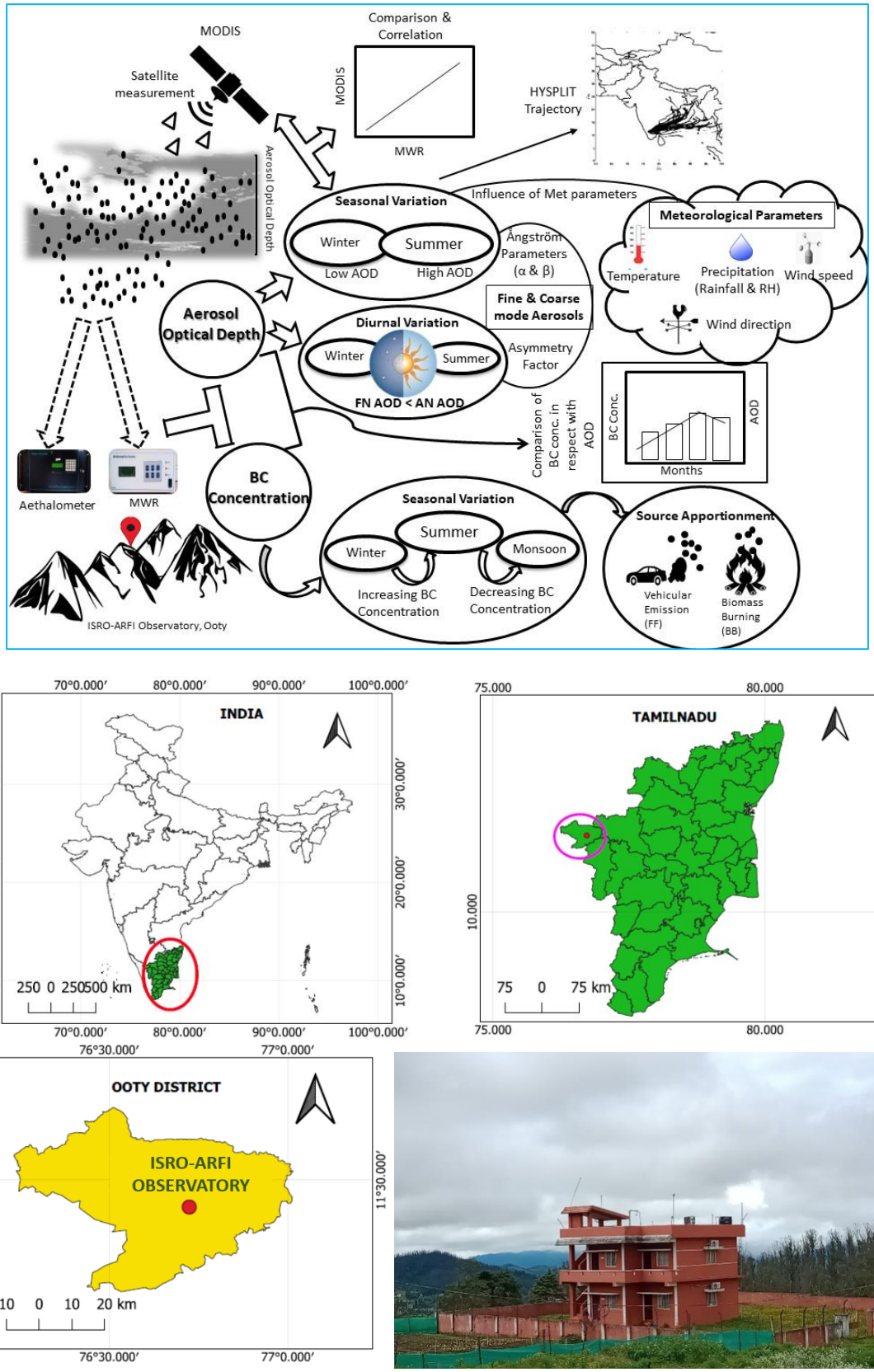

Fig. 1. ISRO-ARFI Observatory at Ooty

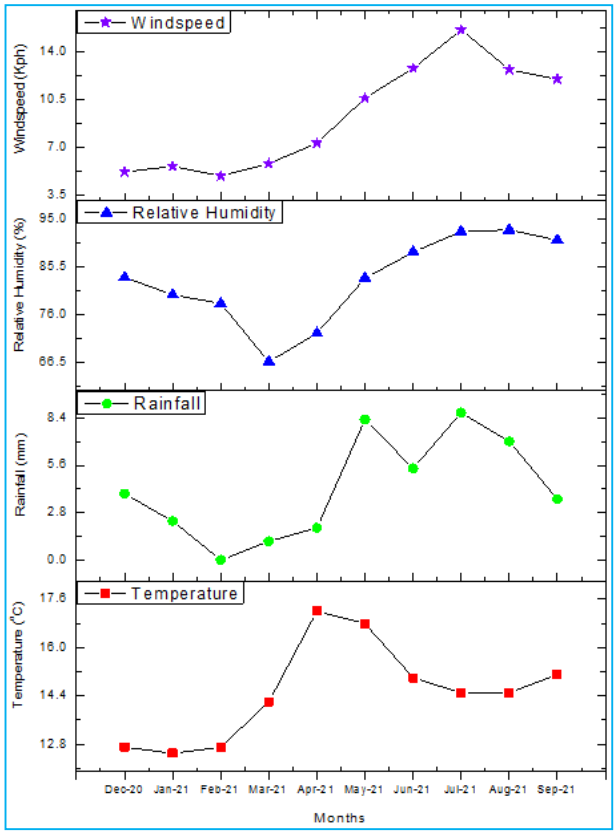

Fig. 2. Meteorological conditions over the study period

categorized into Winter (December 2020 -February 2021), Summer (March 2021 - May 2021), Monsoon (June 2021 - September 2021). The meteorological parameters, like temperature, relative humidity, rainfall, wind speed and wind direction have been recorded for the entire study period (Fig. 2).

The average temperature during the winter season was 12.6 °C with the maximum of 13.4 °C, temperature increases towards the summer season with an average of 16.0 °C and showed a maximum of 17.9 °C, after there was a decline in the temperature increase because of the onset of the monsoon season, which was recorded as 14.7 °C with the maximum of 15.9 °C. The average annual rainfall for the Ooty region was 1200 mms, while comparing all the seasons, Ooty receives high rainfall of 840 mm during the monsoon season with the average of 7.0 mm per rainy day (moderate rain - IMD glossary). The average Relative Humidity during the winter season recorded was 80.8%, summer 74% and the monsoon showed high RH with the average of 91.3% than all other seasons, low temperature, continuous rainfall has been attributed to the increase in relative humidity in this region. The average wind speed during the winter season was 5 kmphs (2.7 knots), during the summer the wind speed was 3 kmphs (1.6 knots) and the monsoon recorded 2 kmph (1.1 knots) revealed the light breeze condition at this study site as per the Beaufort's scale (Jebson, 2007).

2.3. *HYSPLIT Backward-trajectories*

To identify the external sources that contribute to the atmospheric aerosols in the study site, seasonal wise backward trajectories were projected using the Hybrid Single Particle Lagrangian Integrated Trajectory (HYSPLIT) model of the National Oceanic and Atmospheric Administration (NOAA) (Rolph *et al.*, 2017). Trajstat (version 1.2.2.2) software was used to make the trajectory in order to identify possible air mass flow paths and transport of pollutants (Stein *et al.*, 2015). In Trajstat, Latitude, Longitude, Altitude and meteorological data downloaded from NOAA Air Resources Laboratory and other relevant parameters were loaded as an input to make the trajectory of a particular location.

2.4. *Statistical analysis*

The correlation studies were carried out to find the possible correlation of AOD with other dependent variables to assess its dynamic during the study period. MS-Excel was used to estimate the mean and standard deviation of the values. Correlation was performed to find out whether they are related in a positive or in a negative manner that has been revealed by the value ranged between -1.0 to 1.0. A positive correlation was attributed to an increase in both the variables, negative correlation attributed to increases in one value as the other decreases. If the value shows 0, they are not correlated and all are independent.

2.5. *Measurement of Aerosol Optical Depth (AOD)*

The study part consists of the measurement of Aerosol Optical Depth by using the Multi-Wavelength solar Radiometer (MWR) at the ISRO-ARFI observatory venue located at Ooty. The Optical unit of the MWR system was mounted at the rooftop of the observatory building (~10m above ground level) to avoid the deterring of radiation by other topographical objects. Aerosol Optical Depth was studied for the period from December 2020 to May 2021.The Multi-Wavelength solar Radiometer was the ground-based measuring instrument which was designed and developed by Space Physics Laboratory, Vikram Sarabhai Space Centre (SPL, VSSC) based on the filter wheel radiometer's principle (Shaw *et al.*, 1973; Krishna Moorthy *et al.*, 2007). The MWR continuously measures the ground reaching directly transmitting solar flux and spectral extinction at ten

narrow spectral wavelengths, *viz.*, 380, 400, 450, 500, 600, 650, 750, 850, 935 and 1025 nm, allowing the radiation from ultraviolet to the near-infrared region to pass through these filters by an automatic filter wheel motion. Generally, the MWR operated only during clear sky days (Singh *et al.*, 2018). The radiation passes through a field of view (FOV) limited to ∼2◦ using lens pin-hole detector optics, so that the effect of diffuse radiation entering into the FOV on the retrieved optical depths was minimized (Moorthy *et al.*, 1998).

MWR measurements are based on the radiometry principle that follows the Beer- Lamberts-Bouguer law and spectral Aerosol Optical Depth (AOD) is estimated using the Langley technique without the consideration of extra-terrestrial solar flux. According to the flux of solar radiation at the Earth's surface given by Moorthy *et al.* (1999),

$$F_\lambda = F_{0\lambda}\left(\frac{r_0}{r}\right)^2 \exp\left[-\tau_\lambda m\right]$$

where, $F_{0\lambda}$-solar flux at the top of the atmosphere, F_λ-solar flux at the Earth's surface at wavelength λ, r_o-mean Sun–Earth distance, r-instantaneous Sun–Earth distance, τ_λ - Total Optical Depth and m-optical air mass.

MWR converts the above flux into the voltage signal. The output voltage V_λ of the MWR is directly proportional to F_λ at any wavelength (Moorthy *et al.*, 1994),

$$V_\lambda = V_{0\lambda}\left(\frac{r_0}{r}\right)^2 e^{-m\tau_\lambda}$$

Taking natural log on both sides,

$$lnV_\lambda = 1nV_{0\lambda} + 2ln\left(\frac{r_0}{r}\right) - m\tau_\lambda$$

The plot results from the 'm' in *x* axis, ln V_λ in *y*-axis known as the Langley plot and it helps in finding Total Optical Depth (τ_λ). The Langley technique estimates the AOD values by plotting and editing the raw data from the voltage signal (Shaw *et al.*, 1973; Moorthy *et al.*, 2003), the value retrieved as slope of best fit line (Sharma *et al.*, 2012). The values are recorded during both forenoon (0800 AM to 1200 Noon) and afternoon (1201 PM to 0400 PM) hours, which has been considered as a full day data set, other than that partial day (either forenoon or afternoon) AOD values has been recorded every month of the study period.

The sum of several optical depths contributed by the different atmospheric components resulted in the Total Optical Depth (τ_λ),

$$\tau_\lambda = \tau_{R\lambda} + \tau_{g\lambda} + \tau_{w\lambda} + \tau_{a\lambda}$$

where, $\tau_{R\lambda}$-Rayleigh optical thickness, $\tau_{g\lambda}$-Absorption optical depth due to atmospheric gases, $\tau_{w\lambda}$-Water vapor optical depth, $\tau_{a\lambda}$-Aerosol Optical Depth (AOD).

The Aerosol optical depth (AOD) $\tau_{a\lambda}$ was estimated by subtracting the $\tau_{R\lambda}$, $\tau_{g\lambda}$ and $\tau_{w\lambda}$ from

$$\tau_{a\lambda} = \tau_\lambda - \left(\tau_{R\lambda} + \tau_{g\lambda} + \tau_{w\lambda}\right)$$

This $\tau_{a\lambda}$ corresponds to the mean aerosol optical depth for the day (Kumar *et al.*, 2009). Data validation and calibration measurements were done in this present study as mentioned by Moorthy *et al.*, (1999) and Gogoi *et al.* (2008).

2.6. *Spectral Characterization-Ångström exponent and Turbidity coefficient*

The Ångström exponent (α) derived from the spectral distribution of AOD in different wavelengths (λ) was a measure of the relative dominance of fine, submicron aerosols over the coarse aerosols and provides crucial information related to the basic information on the aerosol size distribution (Dhar *et al.*, 2018), whereas the turbidity coefficient (β) represents the measure of total aerosol loading in an atmospheric vertical column (Angstrom, 1961). The formula derived empirically is given as

$$\tau_{a\lambda} = \beta\lambda^{-a}$$

where, $\tau_{a\lambda}$-measured AOD (λ), β-Ångström turbidity coefficient, α-Ångström wavelength exponent

The Ångström parameters α and β were computed in the wavelength interval 380 to 1025 nm by using the log-log scale fit graph of ln AOD vs lnλ nm wavelength. The slope of this graph gives the coefficient α value and the intercept gives β value (Badarinath *et al.*, 2004). Large values of α indicate a relatively high ratio of small to large particles. Value of $\alpha \geq 1.0$ indicate the dominance of fine mode aerosols ($r < 0.5$ μm) over coarse mode (dust and sea salt), whereas, value of $\alpha \leq 1.0$ indicate the dominance of coarse mode aerosols ($r > 0.5$ μm) over fine mode (biomass burning, fossil fuel) (Chatterjee *et al.*, 2012). Value of $\beta < 0.1$ indicates a clean atmosphere, while $\beta > 0.1$ reveals a turbid atmosphere (Singh *et al.*, 2018).

2.7. *Fractional asymmetry factor*

Fractional asymmetry factor (AF) is a factor which gives information about how the forenoon (FN) AODs differ from afternoon (AN) AOD. It gives an idea how the value of AOD changes from morning to evening. It is calculated using the formula suggested by Ganesh *et al.* (2008),

$$\mathrm{AF} = \frac{\mathrm{FN\,AOD} - \mathrm{AN\,AOD}}{\mathrm{FN\,AOD}}$$

2.8. *Measurement of Black Carbon Mass Concentration*

The measurement of Black carbon concentration was carried out using seven channel (370, 470, 520, 590, 660, 880 and 950 nm) Aethalometer instrument (AE-31 Magee Scientific, USA). The aethalometer measures BC concentration based on the principle of the attenuation of a light beam that has transmitted through the sample accumulated quartz fiber filter, which is proportional to the amount of BC loading in the filter (Hansen *et al.*, 1984). The BC measured at the 880 nm wavelength, was considered as a true measure of BC in the atmosphere, at this wavelength other aerosol components have negligible absorption, while BC is the principal absorber of light (Bodhaine, 1995). In the present study, Aethalometer was programmed for recording the attenuation signal for every 5 min, with maintained flow rate at 4 L min^{-1} under standard temperature (T ~ 293°K) and pressure (P_0 ~ 1013 hPa). The ambient pressure was lower than the standard conditions at the high altitude site. Hence, the measured BC values were corrected as mentioned by Moorthy *et al.*, (2004). The true BC mass concentration (M_{BC}) is

$$M_{BC} = M_{BC} * \left[\frac{P_0\,T}{P T_0}\right]^{-1}$$

where, M_{BC}*- Instrument measured raw mass concentration at ambient condition, P_0-Standard pressure, *P*-Ambient pressure, T_0-Standard temperature, *T*-Ambient temperature

2.9. *Absorption properties of BC aerosols*

The values of absorption coefficients were converted to BC mass concentrations by utilizing the "mass-specific absorption cross-section (MAC)", by use this algorithm the absorption coefficient was calculated to make the source apportionment of aerosols. The formula for MAC was,

$$\mathrm{MAC} = \frac{\sigma_{atn}}{C \times R(\mathrm{ATN})}$$

The specific attenuation (σ_{atn}) values of the wavelengths (λ) were mentioned in (Hansen and Schnell (2005). The parameters C and R were the correction factors for minimizing the inherent uncertainty of multiple scattering of light (shadowing effect) in the filter matrix. The correction for these uncertainties was done by incorporating values of C = 2.14 and R = 1 (Weingartner *et al.*, 2003).

2.10. *Calculation of Absorption coefficient*

A power law relation was used to estimate wavelength (λ) dependent absorption coefficient (b_{abs}),

$$b_{abs} \propto \lambda^{-a}$$

where, α - Ångström Exponent

The Ångström exponent was computed by making the exponential curve fitting to a plot of b_{abs} as a function of their respective wavelength (normally between 370 and 950 nm) (Bansal *et al.*, 2019).

The absorption coefficient (b_{abs} or β_{abs}) can be estimated from the BC mass concentrations as,

$$b_{abs} = \frac{\sigma_{atn} \times BC}{C \times R(\mathrm{ATN})}$$

The *BC* concentrations have been classified based on the emission sources like fossil fuel and biomass burning. The emission source was determined by the spectral absorption coefficient (b_{abs}), which is expressed by the Absorption Ångström Exponent (AAE; α),

$$b_{abs} = \beta \lambda^{-a}$$

where, α is an Absorption Ångström exponent and β is a constant.

The two wavelength measurements (370 and 950 nm) were utilized to determine the Absorption Ångström exponent (α), which is an important parameter for aerosol characterization and source apportionment studies (Liu *et al.*, 2018).

The Absorption Ångström exponent of the BC was calculated as suggested by Garg *et al.* (2016),

$$a = -\frac{1n\dfrac{b_{abs}(\lambda_1)}{b_{abs}(\lambda_2)}}{1n\left(\dfrac{\lambda_1}{\lambda_2}\right)}$$

where, λ_1 = 370 nm and λ_2 = 950 nm (Rajesh and Ramachandran, 2017; Kant *et al.*, 2020)

2.11. *Source apportionment of Aerosol*

In this present study, the relative share of biomass burning and Fossil fuel based aerosol was estimated based on the source apportionment of BC component as reported by Sandradewi *et al.*, (2008a) and Sandradewi *et al.*, (2008b) which aims to determine the contribution of biomass from wood burning and fossil fuel from vehicular traffic to the total BC.

The BC concentration originated from fossil fuel (industries, vehicles) and wood burning (forest wildfires, agricultural, waste-material burning, *etc*.,) sources. Hence, it was noted as,

$$BC = BC_{ff} + BC_{bb}$$

The total aerosol absorption coefficient $b_{abs}(\lambda)$ at a particular wavelength can be expressed as the sum of the light absorption of *FF* (fossil fuel - traffic) and BB (biomass burning) sources emitted aerosols (Drinovec *et al.*, 2015; Tiwari *et al.*, 2015);

$$b_{abs}(\lambda) = b_{abs}(\lambda)_{ff} + babs(\lambda)_{bb}$$

Selecting the wavelength pair of 370–950 nm for the b_{abs},

$$b_{abs}(370) = b_{abs}(370)_{ff} + b_{abs}(370)_{bb}$$

$$b_{abs}(950) = b_{abs}(950)_{ff} + b_{abs}(950)_{bb}$$

Using the above equations, the fossil fuel and biomass based absorption coefficients were written as,

$$\frac{b_{abs}(370)_{ff}}{b_{abs}(950)_{ff}} = \left(\frac{370}{950}\right)^{-a_{ff}}$$

$$\frac{b_{abs}(370)_{bb}}{b_{abs}(950)_{bb}} = \left(\frac{370}{950}\right)^{-a_{bb}}$$

The α_{bb} and α_{ff} values were used for this study follow the same values used by several authors (α_{ff} = 1.0-1.1 for fossil fuel and α_{bb} = 1.8-2.0 for biomass burning) in BC source apportionment studies over the Indian region (Rajesh and Ramachandran, 2017; Prasad *et al.*, 2018).

2.12. *Satellite retrieval - Moderate Resolution Imaging Spectroradiometer (MODIS)*

In the present study, MODIS Level-2 (MOD04_L2) product (Terra platform) was used to obtain the daily AOD data at 550 nm at 500 m resolution (Guleria *et al.*, 2012a). The Higher-level MODIS atmosphere products were retrieved through the LAADS web (https://ladsweb.modaps.eosdis.nasa.gov/search/), values were retrieved from the Deep Blue (DB) algorithm (Dhar *et al.*, 2018). The AOD values retrieved from MODIS are accurate within an uncertainty limit of $\Delta\tau_{a\lambda} = \pm 0.05 \pm 0.15\ \tau_{a\lambda}$ over the land, where $\Delta\tau_{a\lambda}$ is the ground-based AOD value (Remer *et al.*, 2005). The data granule was downloaded in the HDF format, and the daily average data was retrieved to the geographical coordinates by using a GIS tool.

2.13. *Interpolation of ground-based measurement to Satellite based measurement*

The Ångström formula were used to interpolate the ground based AOD at 550 nm. The AOD at 550 nm derived from the MODIS was compared with MWR-derived AOD which were interpolated to get the calculated value of ground-based AOD at 550 nm (τ_{550}) (Sharma *et al.*, 2012).

$$\tau_{550} = \tau_{500}\left[\frac{550}{500}\right]^{-a}$$

The value of Ångström wavelength exponent (α) is computed especially for this interpolation in the wavelength interval of 400–750 nm. τ_{500} corresponds to MWR retrieved optical depth at 500 nm (Guleria *et al.*, 2012b).

3. Results and discussion

3.1. *Spectral and monthly variation of Aerosol Optical Depth at different wavelengths*

The Aerosol Optical Depth showed peculiar variation at every respective wavelength during the study period. The data was collected upto the month of May 2021, the available datasets were confined to two seasons. The clear sky days with the full day available datasets for the months of December 2020, January 2021, February 2021, March 2021, April 2021 and May 2021 were 8, 3, 9, 8, 3, 2 days, respectively. The total of clear sky days with full day AOD datasets was 33 days. The partial day (FN or AN) available datasets along with the full day datasets were 46 for the Forenoon and 51 datasets for the Afternoon, totally 97 datasets were available for the entire study period conducted between December 2020 and May 2021.

The AOD values at various wave lengths were tabulated from December 2020 to May 2021

TABLE 1

Monthly Spectral variation of Aerosol Optical Depth (AOD) and its Ångström parameters

Month	380 nm	400 nm	450 nm	500 nm	600 nm	650 nm	750nm	850nm	935nm	1025nm	α	β
Dec 2020	0.200±0.12	0.258±0.21	0.236±0.2	0.206±0.17	0.191±0.13	0.181±0.14	0.112±0.1	0.103±0.1	0.066±0.05	0.064±0.04	1.345	0.076
Jan 2021	0.222±0.13	0.287±0.13	0.232±0.12	0.217±0.11	0.200±0.07	0.165±0.06	0.128±0.04	0.105±0.03	0.093±0.02	0.088±0.02	1.139	0.093
Feb2021	0.189±0.11	0.289±0.12	0.242±0.11	0.217±0.09	0.243±0.11	0.217±0.09	0.137±0.07	0.089±0.04	0.079±0.04	0.071±0.04	1.270	0.086
Mar 2021	0.373±0.25	0.496±0.27	0.421±0.26	0.374±0.26	0.409±0.27	0.362±0.27	0.288±0.26	0.178±0.14	0.216±0.22	0.242±0.21	0.788	0.220
Apr 2021	0.680±0.21	0.660±0.34	0.798±0.32	0.510±0.28	0.678±0.5	0.673±0.46	0.297±0.11	0.410±0.37	0.505±0.47	0.482±0.3	0.523	0.427
May 2021	1.058±0.14	0.963±0.01	0.983±0.11	0.990±0.05	0.850±0.03	0.930±0.05	0.903±0.01	1.055±0.16	1.140±0.26	1.135±0.27	0.100	1.045

(Table 1). The AOD of December, January and February are lower than the subsequent month. The AOD increased at 400 nm and thereafter it started to decrease towards the high wavelength and showed the lowest value at 1025 nm. During February 2021, the AOD showed bimodal peak at both 400 and 600 nm, which indicated the AOD value decreasing as wavelength increases. During March 2021, the AOD peak showed at 400 nm and a decreasing trend towards the higher wavelength and these results were corroborated by the results of Niranjan *et al*., (1997). As mentioned, the optical depth of aerosols gradually decreases from shorter to longer wavelengths up to 600 nm. Afterwards, at 650 nm, there is a minimal increase in optical depth, which then decreases to a minimum at longer wavelengths. According to Junge's inverse power law distribution, the AOD should gradually decline as the wavelength increases. Collectively, the entire winter month experienced the trend of decreasing AOD, with the increasing wavelength. Thus, indicates the loading of abundant fine particles in the atmosphere than coarse particles. This finding was in line with the results of Gogoi *et al*., (2008) where it was mentioned that the AOD spectra was quite steep during the winter season at Dibrugarh, Assam.

On some occasion, the AOD showed an increasing trend at 935 and 1025 nm, the same trend followed in the April month, but the peak shown at 450 nm followed by a sudden drop and rise in values between 500 to 750 nm wavelengths. During May 2021, notable peak and drop of AOD values upto the 750 nm wavelength was observed and from 850 nm onwards, AOD value kick started with an increasing trend, which revealed that the site was dominated by the large sized coarse particles concentration. The result of increasing AOD with the longer wavelength has proven the findings at Kullu valley documented by Sharma *et al*., (2012). The results indicate

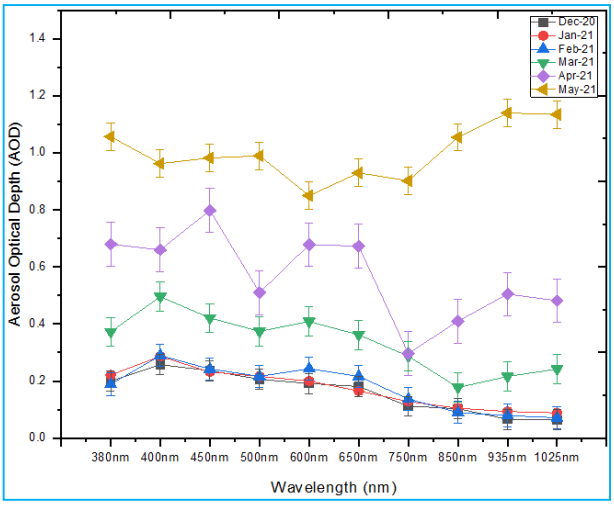

Fig. 3. Spectral variation in Monthly mean Aerosol Optical Depth at different wavelength

that the optical depth was strongly wavelength dependent, thus, the increasing wavelength with diminishing AOD relies the fine particles dominance and vice versa (Kant *et al.*, 2012) (Fig. 3). The results are similar to findings given by Gogoi *et al*., (2009) as higher AOD at 1025 nm compared to 750 nm in May 2007.

3.2. *Seasonal variation of Aerosol Optical Depth*

The daily data sets retrieved from the MWR were converted to the seasonal wise average AOD value for each wavelength. The magnitude of the AOD showed distinct variation over the seasons in respect of the meteorological conditions. The mean AOD value at 500 nm for the Winter was 0.213±0.006 and Summer 0.625±0.323. The result indicated that the AOD was high

TABLE 2

Seasonal variation of Aerosol Optical Depth (AOD) and its Ångström parameters

Month	380 nm	400 nm	450 nm	500 nm	600 nm	650 nm	750nm	850nm	935nm	1025nm	α	β
Winter	0.204±0.017	0.278±0.018	0.237±0.005	0.213±0.006	0.212±0.028	0.187±0.026	0.126±0.013	0.099±0.008	0.079±0.014	0.074±0.013	1.244	0.085
Summer	0.704±0.343	0.706±0.237	0.734±0.286	0.625±0.323	0.646±0.222	0.655±0.285	0.496±0.352	0.548±0.455	0.620±0.473	0.620±0.462	0.223	0.564

TABLE 3

Diurnal variation (forenoon and afternoon) of aerosol optical depth and its ångström parameters

Month/FN	380 nm	400 nm	450 nm	500 nm	600 nm	650 nm	750nm	850nm	935nm	1025nm	α	β
Dec 2020	0.065	0.085	0.056	0.061	0.050	0.053	0.029	0.029	0.029	0.035	0.990	0.029
Jan 2021	0.080	0.145	0.12	0.128	0.102	0.082	0.093	0.088	0.128	0.155	-0.080	0.113
Feb 2021	0.066	0.073	0.064	0.053	0.050	0.045	0.035	0.039	0.048	0.054	0.457	0.041
Mar 2021	0.081	0.128	0.109	0.096	0.090	0.079	0.063	0.062	0.084	0.099	0.309	0.075
Apr 2021	0.353	0.440	0.408	0.324	0.332	0.263	0.208	0.220	0.258	0.353	0.456	0.246
May 2021	1.015	0.955	0.930	1.045	0.670	0.795	0.900	1.145	1.325	1.450	0.310	1.160

Month/AN	380 nm	400 nm	450 nm	500 nm	600 nm	650 nm	750nm	850nm	935nm	1025nm	α	β
Dec 2020	0.269	0.356	0.318	0.285	0.275	0.254	0.166	0.144	0.087	0.074	1.407	0.101
Jan 2021	0.399	0.407	0.333	0.306	0.306	0.266	0.187	0.129	0.111	0.081	1.529	0.106
Feb 2021	0.332	0.463	0.425	0.392	0.413	0.360	0.232	0.155	0.115	0.088	1.473	0.128
Mar 2021	0.632	0.799	0.692	0.624	0.687	0.604	0.464	0.269	0.307	0.331	0.956	0.321
Apr 2021	0.840	1.150	1.125	1.390	1.227	1.140	0.810	1.210	1.470	0.620	0.254	2.099
May 2021	1.100	0.970	1.035	0.935	1.030	1.065	0.905	0.965	0.955	0.820	0.278	3.668

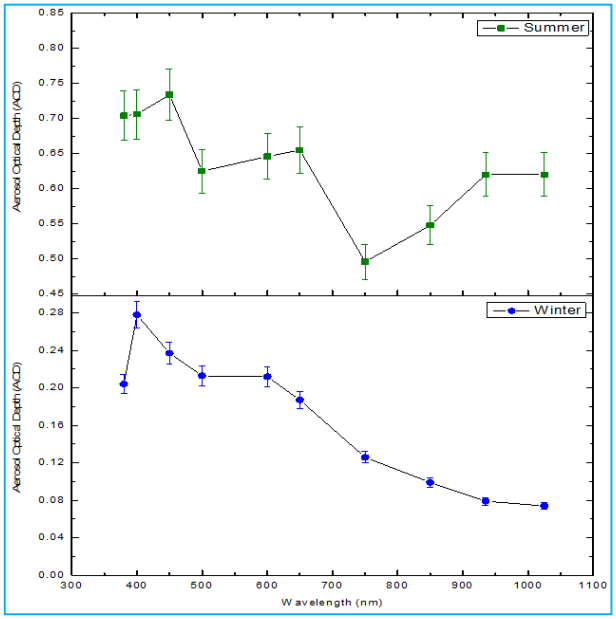

Fig. 4. Seasonal variation of Aerosol Optical Depth at different wavelengths

at the local conditions during the Summer season (Table 2). The Southwest Monsoon kick started during the middle of May 2021 and the datasets for clear sky days were not available thereafter at the study site.

The magnitude of the AOD shows distinct variation over the seasons, thus, the AOD value at 500 nm was recorded lower during the winter while compared with the summer season (Fig. 4). Low AOD levels occur during the winter owing to inefficient generation and gas-to-particle conversion processes, but high AOD occurs during the summer resulting in increased surface heating, which promotes vertical mixing and dust winds. These findings are justified by the results of Kant *et al*., (2012). The AOD might decline during the monsoon season, when actually the MWR recorded values were absent (Sagar *et al.*, 2004). Likewise, in other high-altitude sites reported the AOD values at 500 nm for the summer season over Nanital (0.16-0.45) (~1950 m amsl) (Dumka *et al.*, 2008); over Mohal and in Kullu valley (1154 m msl) (0.24-0.27) (Kuniyal *et al.*, 2009), these results were less similar to the results of Ooty, however, the Ooty site's observations

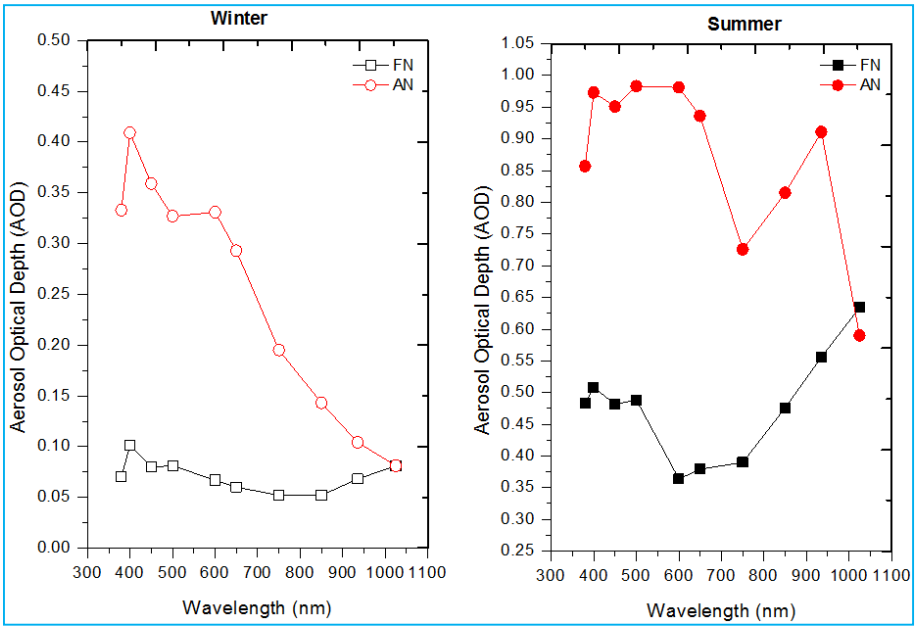

Fig. 5. Diurnal variation of aerosol optical depth during winter and summer

TABLE 4

Asymmetry Factor at different wave length

Month	380 nm	400 nm	450 nm	500 nm	600 nm	650 nm	750nm	850nm	935nm	1025nm
Dec 2020	-3.14	-3.19	-4.69	-3.66	-4.51	-3.76	-4.82	-4.03	-2.01	-1.11
Jan 2021	-3.98	-1.80	-1.78	-1.40	-2.00	-2.24	-1.02	-0.47	0.13	0.47
Feb 2021	-4.03	-5.34	-5.65	-6.39	-7.26	-6.92	-5.64	-3.01	-1.40	-0.62
Mar 2021	-6.78	-5.24	-5.35	-5.50	-6.63	-6.65	-6.37	-3.34	-2.65	-2.34
Apr 2021	-1.38	-1.61	-1.76	-3.29	-2.70	-3.34	-2.90	-4.50	-4.71	-0.76
May 2021	-0.08	-0.02	-0.11	0.11	-0.54	-0.34	-0.01	0.16	0.28	0.43

were similar to the result (0.45-0.62) of low altitude site Hyderabad (~530 m amsl) (Badarinath *et al.*, 2007) for the Summer season. For the winter season, the AOD values were similar to the results noted in low altitude station Rajkot (0.17-0.19) (Ranjan *et al.*, 2007) and high altitude Dibrugarh (0.17-0.38) (Bhuyan *et al*., 2005).

3.3. *Diurnal variation of Aerosol Optical Depth*

The variation in forenoon (FN) and afternoon (AN) has been estimated with monthly and seasonal wise (Table 3). The afternoon AOD values were higher than forenoon AOD values during the entire study period. In all the months, AN AOD was higher than the FN AOD at all the respective wavelengths. As in same, AN AOD seems to be higher at all wavelengths than the FN AOD during both the Winter and Summer season (Fig. 5). The FN and AN variation results in asymmetry factor, that has provided the information regarding the dominance mode of aerosols in the atmosphere.

The convective eddies were developed and strengthened as the increased heating of land with the day advancement. It lifts the particles from the surface below, which eventually break the capping inversion and disperse to higher levels that causing an increasing in the aerosol concentration during afternoon. Similar effects were also reported by Kuniyal *et al*., (2009) at the Kullu site and Himalayan region (Pant *et al.*, 2006).

3.4. *Asymmetry Factor (AF)*

The Asymmetry Factor has been calculated for the study period by using the formula as indicated in Table 4.

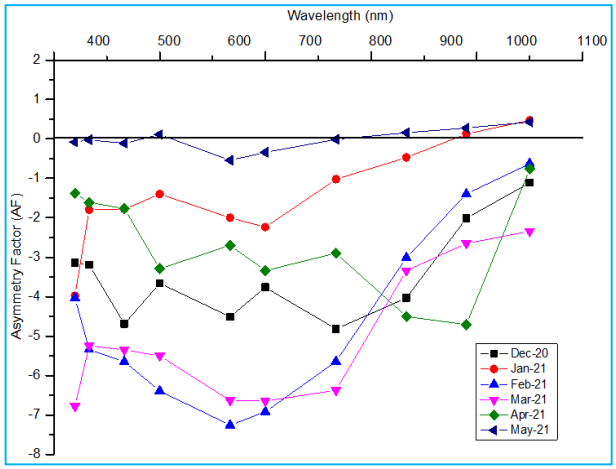

Fig. 6. Asymmetry Factor at different wavelength since December 2020 to May 2021

The values are negative in all the months at all the wavelengths except the January at the wavelengths of 935 and 1025 nm, similarly in the May month some calculated values were positive at the wavelengths of 500, 850, 935 and 1025 nm, respectively.

The negative values indicate an increase in AN AOD. In all the months, the negative AF values were higher at longer wavelengths except in the April month. In both seasons, the AF values were in the negative range and skewed from the longer wavelength to shorter wavelength, and small soaring negative AF values are seen at the near visible region of wavelength (Fig. 6). This result was in line with as noted by Sharma *et al.*, (2012), negative value of AF at Mohal (Kullu valley) implies an increase in AN-AODs, whereas the positive value indicates a decrease in the FN-AODs. Because, evening time becomes more turbid due to day-long increased human activity and vehicular emission along with the convective process at a site. The AF was negative for most of the months at all wavelengths, the reason was similar to the Ooty study site, which noted that the slightly higher in negative AF during the Summer months of April and May, because of the increasing number of tourists and vehicular movements. During almost all the months, the negative AF is maximum at 380 nm and thereafter it drops to its lowest level at 1025 nm, which indicated that more fine particulate matter is produced from forenoon to afternoon during these months (Sharma *et al.*, 2012).

There were several positive values occurred during the winter months, the reason behind that there is low sunlight, resulting in lower overall aerosol generation in the evening and more pollutants capped in a shallow inversion layer in the morning, which breaks with the passage of time due to solar heat and pollutants possibly being convected away by noon and thereafter (McCartney, 1976).

3.5. *Temporal variation of Ångström parameters*

The Ångström parameters were retrieved from the log-log fit scale using the AOD value and its respective wavelength. The mean Ångström Exponent (α) and Turbidity coefficient (β) for December 2020 was 1.345 and 0.076, respectively. During January 2021, it was attributed with the value of 1.139 and 0.093 and February 2021 the Ångström Exponent (α) and Turbidity coefficient (β) were 1.270 and 0.086, respectively. The Ångström Exponent (α) for March 2021 was 0.788 and Turbidity coefficient (β) was 0.220. The Ångström Exponent (α) and Turbidity coefficient (β) were 0.523 and 0.427 (April 2021), 0.100 and 1.045 (May 2021), respectively. The mean Ångström Exponent (α)and Turbidity coefficient (β) for the winter was 1.244±0.237 and 0.085±0.009 respectively, for the Summer season, the mean Ångström Exponent (α) and Turbidity coefficient (β) were 0.223±0.181 and 0.564±0.429, respectively (Table 1 & 2). The mean Ångström Exponent (α) for December 2020, January and February 2021 were higher than 1 ($\alpha>1$), whereas from March to May 2021, the value was less than 1 ($\alpha<1$) and decreasing towards the May month. Collectively, this result indicates the entire study site was attributed to the fine mode aerosols during the Winter and coarse-mode aerosols during the Summer period. Meanwhile, comparing the other months during May, the increasing β value indicates that the site's atmosphere was in turbid condition. Niranjan *et al.*, (1997) has observed the same results in line with results observed at Ooty site. The turbidity coefficient (β) is higher in May, which indicated higher pollution levels through all the Summer months.

In winter, high α value revealed that the abundance of fine-mode and absorbing aerosols due to anthropogenic activities nearby industrialized town settlements. This was also similar to the results reported at the Agartala site documented by Dhar *et al.*, (2018) found highly polluted Indo-Gangetic Plains (IGP) and industrialized northern part of India.

The AOD was negatively related to the derived Ångström Exponent (α), meanwhile, it was highly correlated with the Turbidity coefficient (β) at the entire study period (Fig. 7). The AOD has a strong negatively correlation with the Ångström Exponent (α) with the correlation coefficient value of R = -0.79 meanwhile, it has a strong positive correlation with the Turbidity coefficient (R = 0.99). Notably, the Ångström Exponent (α) has strong negative correlation with the Turbidity

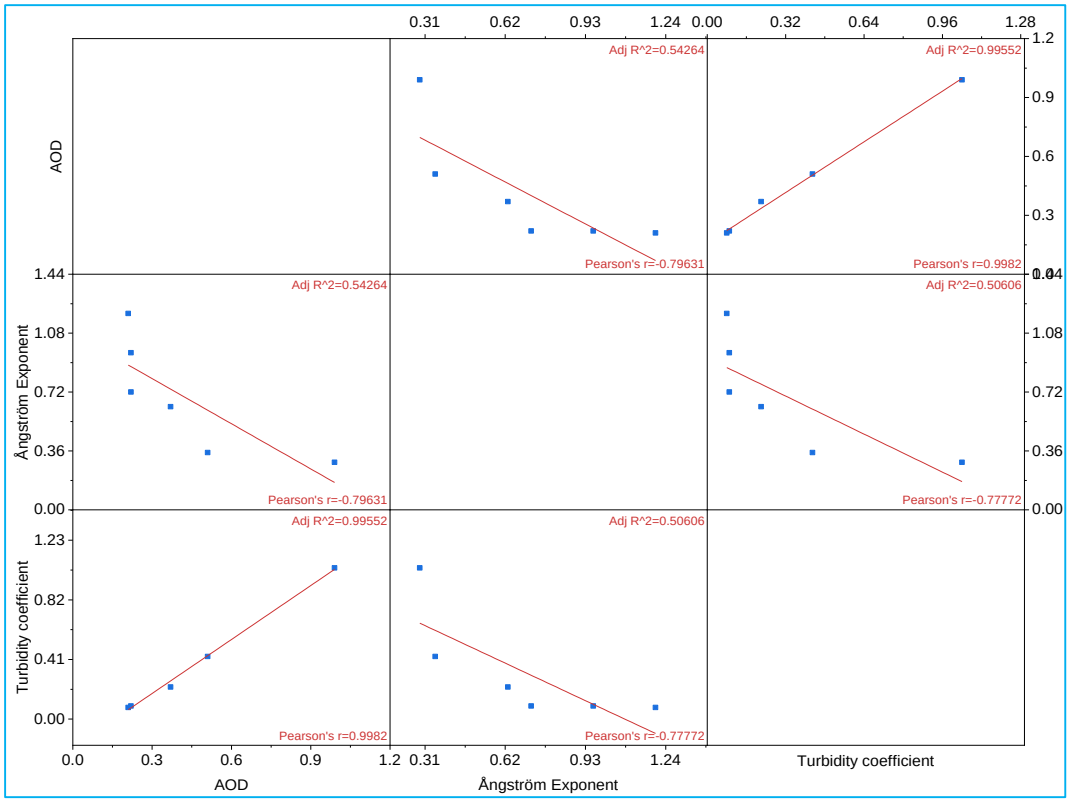

Fig. 7. Correlation between the Monthly Aerosol Optical Depth, Ångström Exponent (α) and Turbidity coefficient (β)

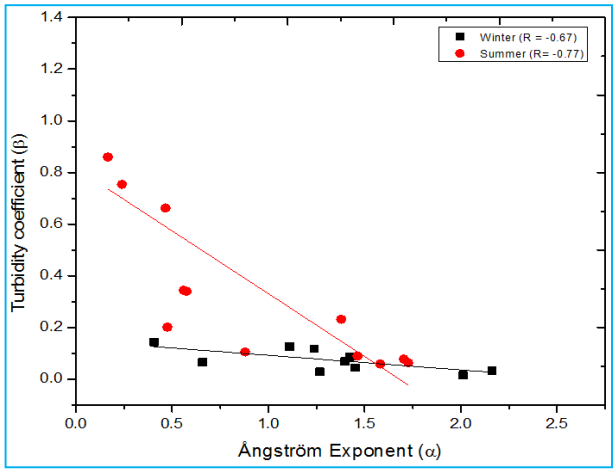

Fig. 8. Correlation between the Seasonal Ångström Exponent (α) and Turbidity coefficient (β)

TABLE 5

Comparison of Aerosol Optical Depth and Black Carbon (BC) Concentration

Month	AOD (500 nm)	BC (μg m^{-3})
Dec 2020	0.206	0.325
Jan 2021	0.217	0.437
Feb 2021	0.217	1.340
Mar 2021	0.374	1.466
Apr 2021	0.510	1.448
May 2021	0.990	0.425
Jun 2021	NA	0.197
Jul 2021	NA	0.163
Aug 2021	NA	0.157
Sep 2021	NA	0.222

NA – Not Available

coefficient (β) (R = -0.78) and this was due to the increasing fine mode aerosols (as the increased α value) lead to decrease in the atmospheric turbid condition (β). These results were in line with the findings of Schuster *et al*., (2006). Collectively, during the entire study period as β increases, Ångström Exponent (α) decreases, which relies that α was negatively correlated with the Turbidity coefficient (β) and this trend was found similarly to both the Winter (Correlation coefficient R = -0.67) and Summer (Correlation coefficient R = -0.77) seasons (Fig. 8). This indicates that as the increase in aerosol

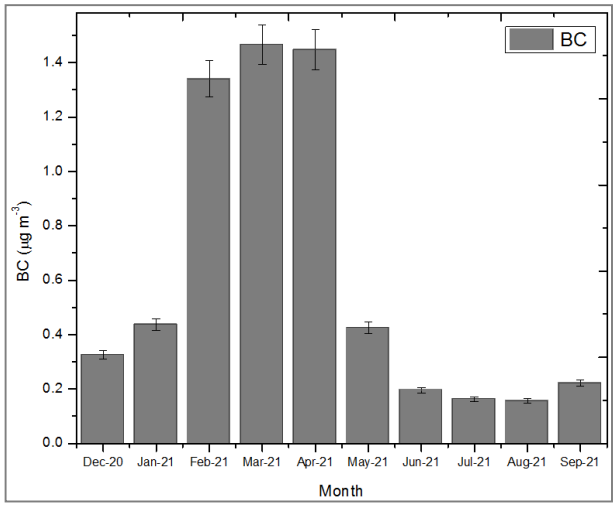

Fig. 9. Monthly Black Carbon (BC) concentration (µg m^{-3})

loading (coarse aerosol particles) enhance the turbidity level, decrease the dominance of fine aerosol (Sagar *et al.*, 2004).

3.6. *Monthly and Seasonal variation Black Carbon (BC) concentration*

The Black Carbon mass concentration was measured along with the measurement of ground-based AOD simultaneously. Despite the absence of AOD measurements due to insufficient solar intensity during the Monsoon months of June to September 2021, BC measurements were taken till September 2021 (Table 5). Accordingly, BC concentrations were measured, recorded and retrieved for the three seasons of Winter, Summer, and Monsoon. The average BC mass concentration for the Winter and Summer were estimated as 0.680±0.206 µg m^{-3} and 1.128±0.393 µg m^{-3} while during Monsoon it was 0.189±0.06 µg m^{-3}.

The Black Carbon mass concentration has increased from January and attained the peak during April, thereafter it has started to decline in concentration from June onwards (Fig. 9). This result was in accordance with the previous studies of Kowsalya *et al*., (2020) and Udayasoorian *et al*., (2014a). The seasonal BC concentration has a significant dynamic trend over the study period and the concentration showed an increasing trend towards summer and then the concentration receded during the Monsoon season. The concentration of the BC observed was in line with the results of Raju *et al*., (2020) where they noted that the Mahabaleshwar site recorded the value of 1.50 ± 0.64 µgm^{-3} during Summer and Monsoon (0.45 ± 0.39 µg m^{-3}), however, the high concentration attributed to season was varied. The results

TABLE 6

Seasonal Black Carbon concentration and its Source apportionment

Seasons	BC_{bb}	BC_{ff}	BC
Winter (Dec-Feb)	0.001	0.679	0.680 ± 0.206
Summer (Mar-May)	0.001	1.127	1.128 ± 0.393
Monsoon (Jun-Sep)	0.001	0.188	0.189± 0.06

of the Ooty study site was very low in all seasons while comparing with the results of Kodaikanal (more or less with the same altitude ~ 2311 m amsl) during the Winter (2.58 ± 0.15 µg m^{-3}), Summer (1.98 ± 0.19 µg m^{-3}) and Monsoon (1.01 ± 0.19 µg m^{-3}), because the Ooty study site was farther from industrialized and anthropogenic activity regions. The Summer peak was occurring due to the high temperature that deepens the boundary layer along with surface layer breakup and BC aerosols were brought by convection and prevailing north easterlies and easterlies wind from surrounding valley region to the observation site, which led to increased BC concentration (Raju *et al.*, 2020). The concentration of BC was significantly declined during the Monsoon season because of the scavenging activity washed out by the rainfall (Guha *et al.*, 2015).

3.7. *Monthly and Seasonal Source Apportionment of Black Carbon (BC) aerosol*

The sources of Black Carbon aerosol are apportioned, whether they are dominated by fossil fuel based or by biomass burning based aerosols. As the result indicated that the Black carbon source was purely dominated by fossil fuel-based soot particles, the biomass burning based particles sparsely contributed to the total mass concentration during the entire study period. The biomass-based soot particles contribution was in the range of 0.001 µg m^{-3} in all the seasons, the contribution of the fossil fuel-based BC were 0.679 µg m^{-3}, 1.127 µg m^{-3} and 0.188 µg $m^{-3}$for the Winter, Summer and Monsoon seasons, respectively (Table 6).

The source apportionment of Black Carbon results depicts a clear view of the source of loading the BC concentration over the study site. The sources for the total BC were divided based on fossil fuel based and biomass burning. At Ooty study site during the entire study period, the BC concentration was dominated by fossil fuel based sources (BC_{ff}) and biomass burning based sources were contributed at a very meagre level (BC_{bb}). The contribution level of BC_{bb} was confined within the range

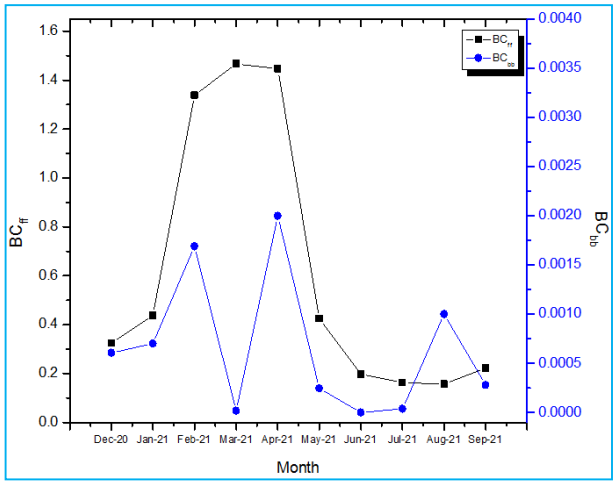

Fig. 10. Source apportionment of Black Carbon aerosol (BC_{ff} and BC_{bb})

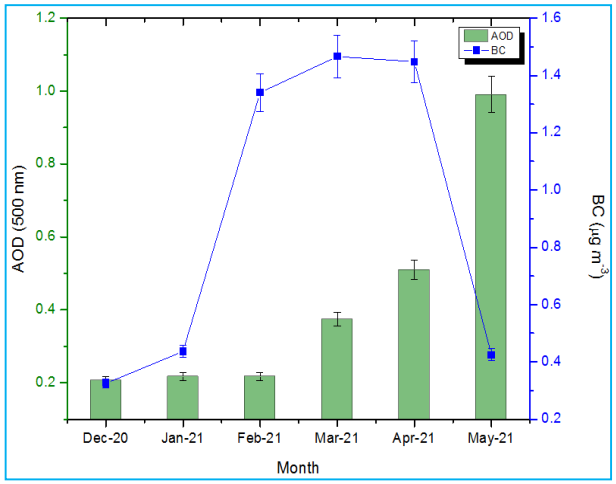

Fig. 11. Monthly comparison of Black Carbon (BC) concentration with the Aerosol Optical Depth at 500 nm

of 0 to 0.002 µg m^{-3} (Fig. 10). Notably, in all the seasons the fossil fuel based BC was dominated over the biomass burning based particles to the total BC concentration. This result concluded that Ooty study site was dominated by fossil fuel burning particles. This result was corroborated by the Absorption Ångström Exponent (AAE) value ($\alpha \leq 1.1$) denotes the fossil fuel based source (Rajesh and Ramachandran, 2017). This result was similar to the findings of past studies conducted by Udayasoorian *et al*., (2014b) and Gogoi *et al*., (2021). The enhanced contribution of BC_{ff} to the total BC concentration was significantly higher than the BC_{bb} during all the seasons and the findings are corroborated by Vaishya *et al*., (2017) where they indicated the variation in contribution percentage was comparatively higher. The contribution of BC_{ff} concentration was found to be high during Winter and Monsoon due to a significant increase in industrial activities and vehicular movement, occurrence of shallow atmospheric layer and low wind speed that traps the particulate matter near the surface (Rajesh and Ramachandran, 2017). During the Summer season, the contribution of the BC_{ff} was found to be higher due to more visiting tourists and vehicular movement near to the study site. Meanwhile the Winter and Monsoon season experience less vehicular movement accompanied with the washing out of Aerosols which comparatively reduced the BC concentration. The findings of Bhaskar *et al*., (2018) supported this result.

3.8. *Comparison of Aerosol Optical Depth with the Black Carbon (BC) concentration*

In the aerosol optical properties, BC possess peculiar optical properties in terms of extinction of radiation and thus, the BC contribute to the Aerosol Optical Depth. The AOD and BC concentration was 0.206 and 0.325 µg m^{-3} (December 2020); 0.217 and 0.437 µg m^{-3} (January 2021); 0.217 and 1.340 µg m^{-3} (February 2021); 0.374 and 1.466 µg m^{-3} (March 2021); 0.510 and 1.448 µg m^{-3} (April 2021), 0.990 and 0.425 µg m^{-3} (May 2021), respectively.

In the aerosol optical properties, BC possesses peculiar optical properties in terms of extinction of radiation, thus, the BC contributes to the Aerosol Optical Depth. The Ångström Exponent (α) values denoted that the Ooty study site was dominated by fine mode aerosols during the Winter season and coarse mode aerosols during the Summer season. The aerosol Black Carbon (BC), one of the fine mode aerosols, may contribute to the Aerosol Optical Depth at the study site. The BC concentration was increasing with the increasing AOD trend for each month, this trend followed for the entire winter period. This result trend was similar to the results of Sinhagad site, where the BC significantly contributed to the AOD during the Winter season, reported by Safai *et al*., (2014). However, during the summer, especially during the May month, the BC concentration was low, even though the AOD was high (Fig. 11). This is because of the occurrence of rainfall (8.3 mm) during the middle of the May month that has washed out the Black Carbon and AOD measurements has been temporarily stopped within the initial week of the month due to lack of ample sunlight associated with the kick-started Southwest monsoon.

3.9. *Comparison of ground based AOD and Satellite retrieved AOD*

Ground measured AOD was compared with the satellite retrieval AOD value. The daily AOD value was retrieved from the MODIS as to the data sets available for

TABLE 7

Monthly meteorological parameters

Months	Temperature (°C)	Cumulative Rainfall (mm)	Relative Humidity (%)	Wind speed (kmph)	Wind Direction (o)
Dec 2020	12.7	120.6	83.4	5	95.6
Jan 2021	12.5	71	80.0	6	107.2
Feb 2021	12.7	0.0	78.2	5	112.6
Mar 2021	14.2	34.7	66.6	6	109.6
Apr 2021	17.2	56.4	72.3	7	148.9
May 2021	16.8	257.8	83.3	11	186.2

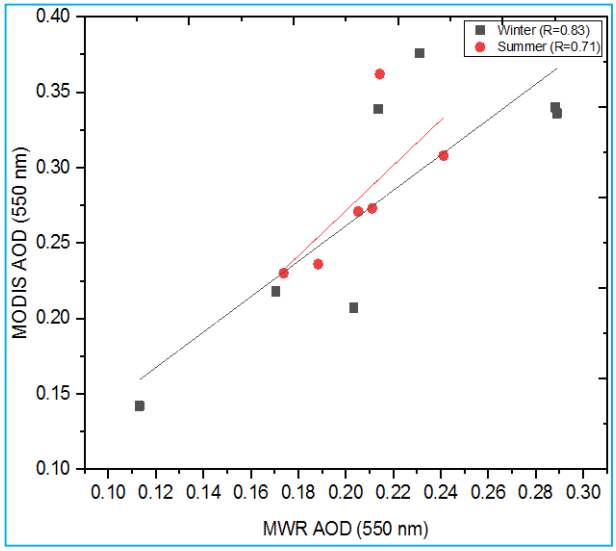

Fig. 12. Comparison of MWR measured Aerosol Optical Depth with MODIS retrieved Aerosol Optical Depth during Winter and Summer

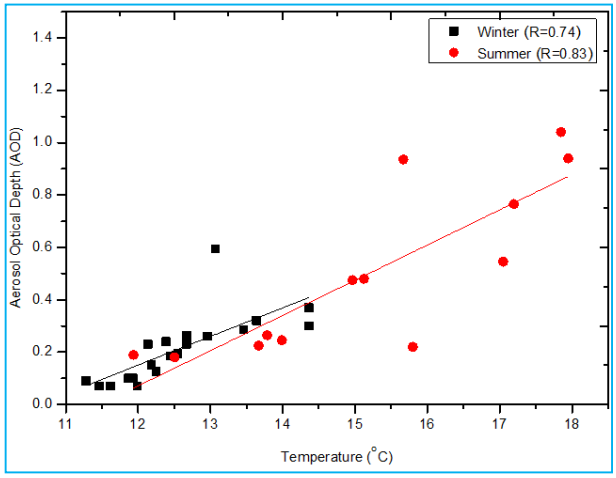

Fig. 13. Influence of Seasonal Temperature on the Aerosol Optical Depth

the study period, other than that, the monthly mean AOD was retrieved from the MERRA-2 to validate it with the ground measured monthly AOD value. The measured value at 500 nm has been interpolated to the 550 nm for the comparison of ground-based value to the satellite retrieval value.

The ground based AOD has a good correlation with the MODIS retrieved value during the Winter season with a correlation coefficient of R = 0.83 and marginally correlated during the Summer season with the correlation coefficient of R = 0.71 (Fig. 12). The authors Singh *et al.*, (2020) make comparison of MWR measured AOD with MODIS retrieved AOD, which has been well correlated with a correlation coefficient of 0.70 (Winter) and 0.57 (Summer). This finding was reasonably similar to Ooty site's results. The deviation from the ground measured AOD has been already discussed by several authors, systematic deviation between satellite and ground-based observations reported by Jing-Mei *et al.*, (2010) and Guleria *et al.*, (2012b). They noted that the occurrence of deviation slope and systematic biases were mainly due to the aerosol model assumptions in the MODIS algorithm.

3.10. *Influence of meteorological parameters on Aerosol Optical Depth*

Atmospheric loading aerosols were supposed to the dynamics of the synoptic conditions, thus, Aerosol Optical Depth is also influenced by the daily meteorological parameters. The meteorological parameters were retrieved from the automatic weather station available at the observatory and the monthly average values of the temperature, relative humidity, rainfall, wind speed and wind directions were tabulated (Table 7).

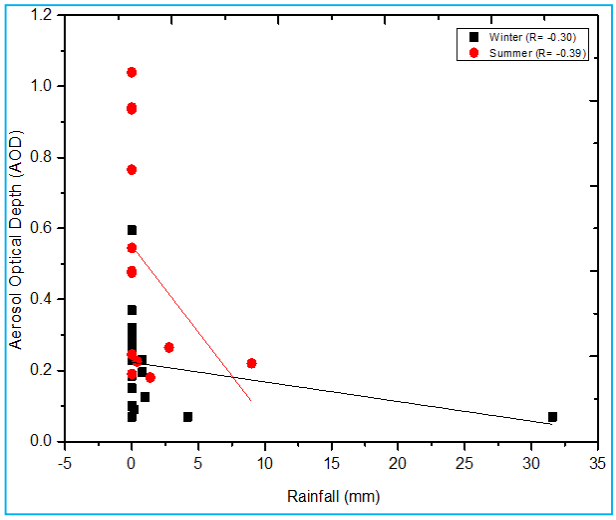

Fig. 14. Influence of Seasonal Rainfall on the Aerosol Optical Depth

The meteorological parameters like temperature, relative humidity, rainfall, wind speed and wind direction were influencing the atmospheric aerosols. Thus, the Aerosol Optical Depth was supposed to the dynamic meteorological parameters. The values of Aerosol Optical Depth taken at 500 nm for the influence study of meteorological parameters.

3.11. *Influence of Temperature on Aerosol Optical Depth*

The temperature influenced the Aerosol Optical Depth temporally. The Aerosol Optical Depth was positively correlated with the temperature during the Winter (R = 0.74) and Summer (R = 0.83) seasons (Fig. 13). During the Winter season, due to weak convection and steep boundary layer, the atmospheric vertical column is attributed to increased aerosol concentration and a high AOD. The findings of Sharma *et al*., (2012) also noted, similar results in this study that the positive relation of temperature with AOD during Winter months.

Higher AOD in Summer may be attributed to the prevailing of high surface wind than other seasons. The soilderived dust aerosols were lofted by the prevailing wind from the surface, thereafter, the concentration was higher during the Summer season. This fact has been discussed by Pathak *et al*., (2010) at dry lands of the Brahmaputra River basin. The author Reddy *et al*., (2016) noted the reason for high AOD as the increased surface temperature during summer may leads to enhanced photochemical process that stipulated the aerosol hygroscopic growth and leads to the formation of secondary aerosol.

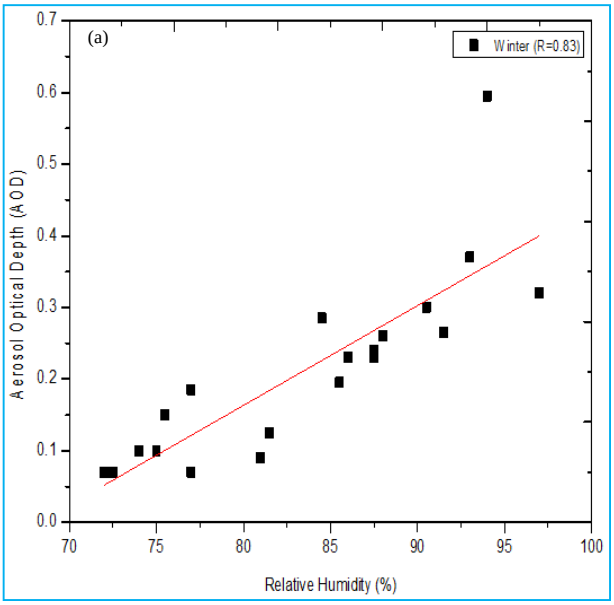

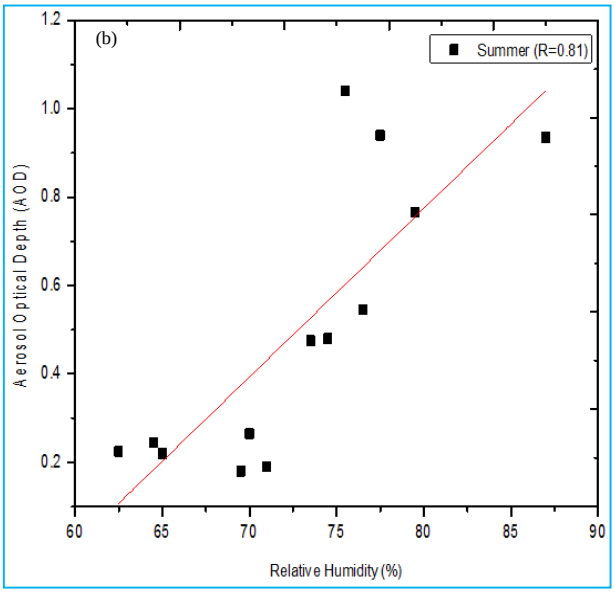

Figs. 15(a&b). Influence of Relative Humidity on the Aerosol Optical Depth (a) Winter and (b) Summer

3.12. *Influence of Rainfall on Aerosol Optical Depth*

The seasonal rainfall occurrence has significantly affected the aerosol loading in the atmosphere. The Aerosol Optical Depth was negatively correlated with the rainfall at both the seasons of Winter (R = -0.30) and Summer (R = -0.39) (Fig. 14), which indicated that the occurrence of rainfall might wash out the atmospheric loading aerosols. Bhaskar *et al*., (2018) discussed same observation had proven the influence of rainfall on aerosols.

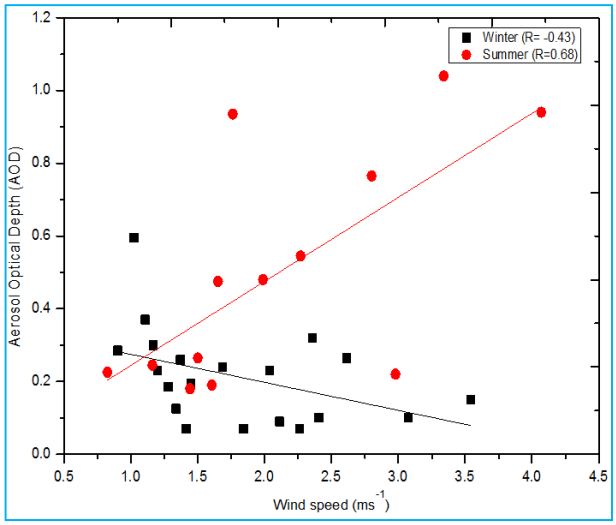

Fig. 16. Influence of Wind speed on the Aerosol Optical Depth

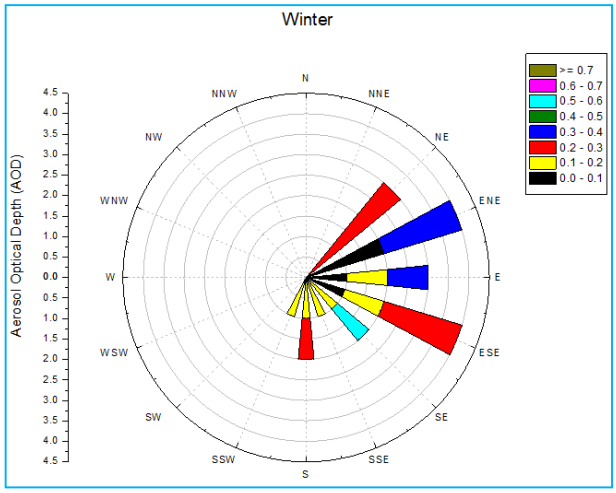

Fig. 17. Influence of Wind direction on the Aerosol Optical Depth during Winter

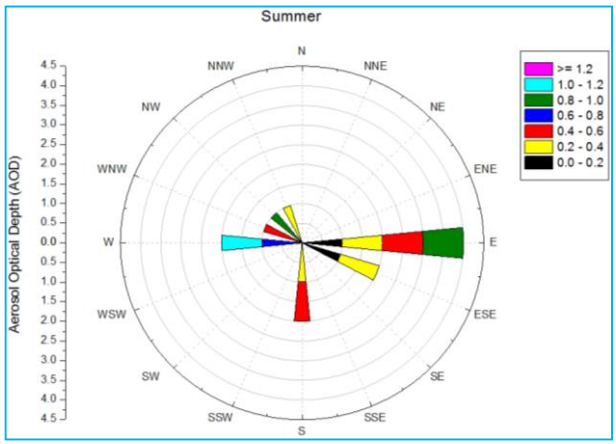

Fig. 18. Influence of Wind direction on the Aerosol Optical Depth during Summer

3.13. *Influence of Relative Humidity on Aerosol Optical Depth*

The result showed that the Relative Humidity (RH) was strongly correlated with the AOD in both the Winter and Summer season where the correlation coefficients were R = 0.83 and R = 0.81, respectively [Figs. 15(a&b)]. Even though the rainfall reduced the near-surface aerosol concentration, whenever the RH increases significantly, the AOD also increases and this might be due to the hygroscopic growth of water-soluble aerosols. The high ambient RH results in growth of coarse mode aerosols and water-soluble fine mode aerosols which leads to high AOD in the Summer season, whereas the AOD is slightly lower during winter than the summer and associated with the fine mode particles (Balakrishnaiah *et al.*, 2011).

3.14. *Influence of Wind speed on Aerosol Optical Depth*

Aerosols were originated on one site and transported for vast distances by wind systems resulted in effects at particular locations that were far away from the source (Kumar *et al.*, 2009). The Aerosol Optical Depth was negatively correlated to the Wind speed during the Winter season (R = -0.43), whereas it has a positive correlation during the Summer season (R = 0.68) (Fig. 16). The negative correlation denoted that the increase in wind speed led to a decrease in Aerosol Optical Depth, which were corroborated by the findings of Rana *et al.*, (2009), who observed that the lower AOD values at the high altitude station with a mean wind speed of ~2 m/s during the Winter season. The positive correlation showed the increase in Wind speed led to enhanced AOD, which may be attributed to prevailing high surface wind during the summer which have lofted the surface aerosols and dust from the valley towards the study site (Sharma *et al.*, 2012), along with this loading of marine aerosols that have been transported towards the wind by through the westerlies wind. Hence, the concentration was higher during the Summer season over the study site.

3.15. *Influence of Wind direction on Aerosol Optical Depth*

The wind rose graph showed the direction of wind flow, which indicates that the winter was attributed to the North-east and Easterly winds and then summer was attributed with the Easterly, Westerly and North-westerly winds (Figs. 17&18). This wind rose graph represents the sources of aerosols from where they come towards the

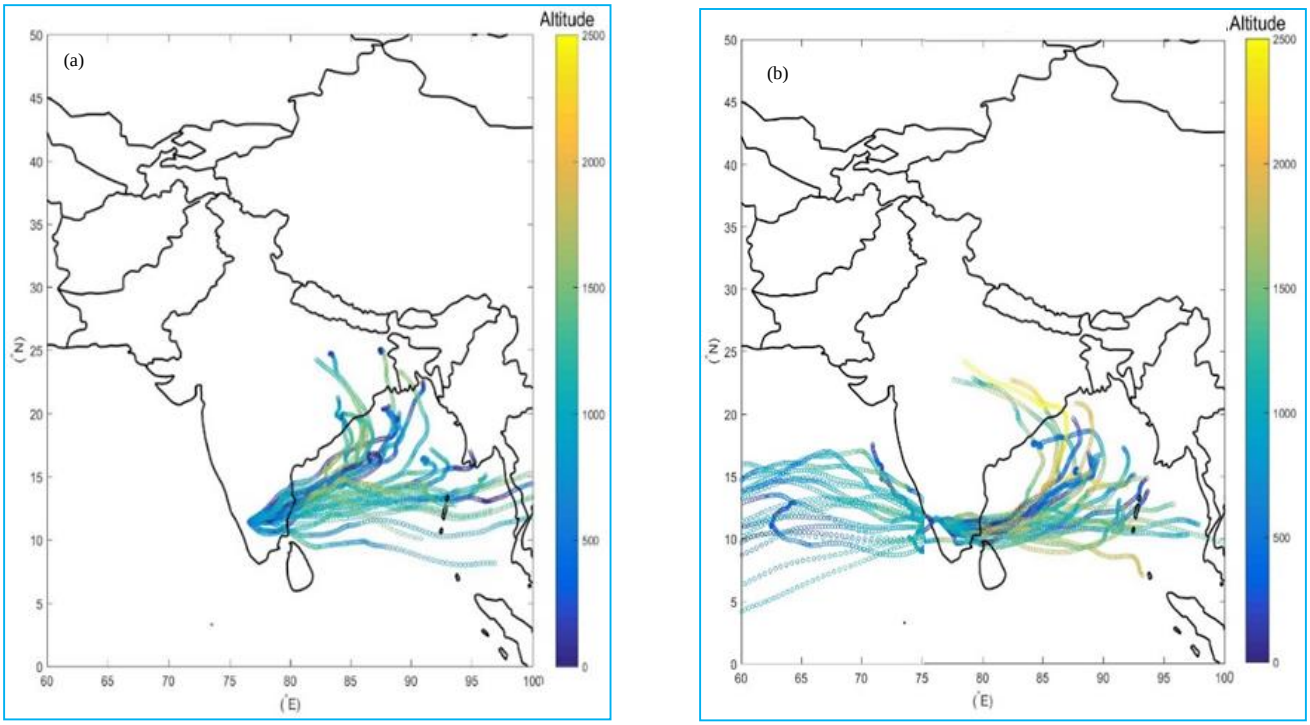

Figs. 19(a&b). HYSPLIT trajectory of the study site during (a) Winter (December, 2020 to February, 2021) and (b) Summer (March to May, 2021)

site, which gave the view on the continental as well as the marine aerosols as with the direction. The wind direction pattern for this study site has already been discussed by Udayasoorian *et al*., (2014b) and Kompalli *et al*., (2018).

3.16. *HYSPLIT Backward Trajectory*

To determine the loading of aerosols at the study site by its transport from another source region, the HYSPLIT trajectory was plotted. This indicates the transport of aerosols over the continental and marine regions and its dynamic direction during each month and shows the monthly trajectory, which was combined as the seasonal wise trajectory (Winter and Summer) (Fig. 19). Thus, the Aerosol Optical Depth at the study site was contributed by the several aerosols that were transported from various regions to the study site during all the seasons.

In concern the determination of aerosol transportation, HYSPLIT Backward trajectory has plotted from 0 to 2500 m amsl, the study was located at 2500 m amsl. During the Winter, the trajectory denoted the sources from the continental site, along with high α value indicated abundance of fine mode aerosols (Carbonaceous aerosols). The air masses were blown from the North and North-easterly winds and some sources were from the South easterly wind during the Winter. Whereas during the summer the trajectory denoted that the sources were from the continental and marine origin, the trajectory lies in the North and North-westerlies, some may also from the easterly side. The Summer season has a low α value indicates the abundance of coarse mode aerosols (sea salt and dust). The trajectory plot and then wind rose also projected the same wind direction, the mode of aerosols was also in line with the determined results.

With the view on trajectory, the easterly advection was predominantly over the Winter and the initial month of the Summer season that revealed the air masses may carry aerosols from the Metropolitan cities like Chennai and Bangalore, South-easterly winds may carry the particles from the nearby city of Coimbatore and contribute more to the AOD at this site. The westerly winds may carry sea salt aerosols that originated from the Arabian sea and dust particles from the nearby cities. The North-westerly winds predominantly during the Summer season may contribute the aerosols to AOD from the nearby cities like Kozhikode and Mangalore along with marine originated sea salts. The advection and source of transportation towards this site had been discussed by Udayasoorian *et al*., (2014b).

4. Conclusion

Based on the research findings, it was concluded that AOD is wavelength dependent, monthly and seasonally

varied. The AOD was higher during AN than the FN during all the seasons. The site was dominated by fine mode aerosols during the winter and coarse mode aerosols during the Summer. Among the fine mode aerosols, BC was significantly contributed to the AOD. The concentration of the BC was attributed to the more fossil fuel based particles. Local prevailing meteorological parameters had significantly affected the AOD, parameters like temperature, relative humidity and wind speed (during summer alone) were positively correlated with the AOD, rainfall and wind speed (during winter alone) showed a negative correlation with the AOD. The North-easterlies and Easterly winds contributed continental aerosols to the AOD during the Winter, North-westerlies and Westerly winds contributed to the marine and continental origin aerosols to the AOD during the Summer. Despite the fact that the site is clean, the AOD linked with aerosol concentration showed the long-distance movement of aerosols from the nearby towns and cities and contributed to the total AOD at this study site, which may due to the effect of meteorological factors.

Acknowledgement

This study was carried out under the Aerosol Radiative Forcing over India (ARFI) project of the ISRO-GBP programme. The authors are grateful thanks to the Space Physics Laboratory, Vikram Sarabhai Space Centre (VSSC), Indian Space Research Organization (ISRO) for providing opportunities for their research project, and for their logistic support and funding to the entire part of the study.

Conflict of Interest : The authors declare that they have no conflict of interest.

Disclaimer : The contents and views expressed in this study are the views of the authors and do not necessarily reflect the views of the organizations they belong to.

References

Ångström, A., 1961, "Determinig the Turbidity of the Atmosphere", *Tellus*, XIII.

Badarinath, K., Kharol, S. K., Latha, K. M., Chand, T. K., Prasad, V. K., Jyothsna, A. N. and Samatha, K., 2007, "Multiyear ground-based and satellite observations of aerosol properties over a tropical urban area in India", *Atmospheric Science Letters*, **8**, 1,7-13.

Badarinath, K., Latha, K. M., Chand, T. K., Gupta, P. K., Ghosh, A., Jain, S., Gera, B., Singh, R., Sarkar, A. and Singh, N., 2004, "Characterization of aerosols from biomass burning-a case study from Mizoram (Northeast), India", *Chemosphere*, **54**, 2, 167-175.

Balakrishnaiah, G., Reddy, B. S. K., Gopal, K. R., Reddy, R., Reddy, L., Ahammed, Y. N., Narasimhulu, K., Moorthy, K. K. and Babu, S. S., 2011, "Analysis of optical properties of atmospheric aerosols inferred from spectral AODs and Ångström wavelength exponent", *Atmospheric Environment*, **45**, 6, 1275-1285.

Bansal, O., Singh, A. and Singh, D., 2019, "Characteristics of Black Carbon aerosols over Patiala Northwestern part of the IGP: Source apportionment using cluster and CWT analysis", *Atmospheric Pollution Research*, **10**, 1, 244-256.

Bhaskar, B.V., Rajeshkumar, R., Muthuchelian, K. and Ramachandran, S., 2018, "Spatial, temporal and source study of black carbon in the atmospheric aerosols over different altitude regions in Southern India", *Journal of Atmospheric and Solar-Terrestrial Physics*, **179,** 416-424.

Bhuyan, P., Gogoi, M. and Moorthy, K. K., 2005, "Spectral and temporal characteristics of aerosol optical depth over a wet tropical location in North East India", *Advances in Space Research*, **35**, 8, 1423-1429.

Bodhaine, B. A., 1995, "Aerosol absorption measurements at Barrow, Mauna Loa and the south pole", *Journal of Geophysical Research: Atmospheres*, **100**, D5, 8967-8975.

Chatterjee, A., Ghosh, S. K., Adak, A., Singh, A. K., Devara, P. C. and Raha, S., 2012, "Effect of dust and anthropogenic aerosols on columnar aerosol optical properties over Darjeeling (2200 m asl), eastern Himalayas, India", *PloS one*, **7**, 7, e40286.

Dhar, P., Banik, T., De, B. K., Gogoi, M. M., Babu, S. S. and Guha, A., 2018, "Study of aerosol types and seasonal sources using wavelength dependent Ångström exponent over North-East India: ground-based measurement and satellite remote sensing", *Advances in Space Research*, **62**, 5, 1049-1064.

Drinovec, L., Močnik, G., Zotter, P., Prévôt, A., Ruckstuhl, C., Coz, E., Rupakheti, M., Sciare, J., Müller, T. and Wiedensohler, A., 2015, "The 'dual-spot' Aethalometer: an improved measurement of aerosol black carbon with real-time loading compensation", *Atmospheric measurement techniques*, **8**, 5, 1965-1979.

Dumka, U., Moorthy, K. K., Pant, P., Hegde, P., Sagar, R. and Pandey, K., 2008, "Physical and optical characteristics of atmospheric aerosols during ICARB at Manora Peak, Nainital : A sparsely inhabited, high-altitude location in the Himalayas", *Journal of earth system science*, **117**, 1, 399-405.

Ganesh, K., Umesh, T. and Narasimhamurthy, B., 2008, "Site specific aerosol optical thickness characteristics over Mysore", *Aerosol and Air Quality Research*, **8**, 3, 295-307.

Garg, S., Chandra, B. P., Sinha, V., Sarda-Esteve, R., Gros, V. and Sinha, B., 2016, "Limitation of the use of the absorption angstrom exponent for source apportionment of equivalent black carbon : a case study from the North West Indo-Gangetic Plain", *Environmental science & technology*, **50**, 2, 814-824.

Gogoi, M., Bhuyan, P. and Moorthy, K. Krishna, 2008, "Estimation of the effect of long-range transport on seasonal variation of aerosols over northeastern India", *Annales Geophysicae.*

Gogoi, M. M., Moorthy, K. Krishna, Babu, S. S. and Bhuyan, P. K., 2009, "Climatology of columnar aerosol properties and the influence of synoptic conditions : First-time results from the northeastern region of India", *Journal of Geophysical Research: Atmospheres*, **114**, D8.

Gogoi, M. M., Babu, S. Suresh, Arun, B., Moorthy, K. K., Ajay, A., Ajay, P., Suryavanshi, A., Borgohain, A., Guha, A. and Shaikh, A., 2021, "Response of ambient BC concentration across the Indian region to the nation-wide lockdown : results from the ARFINET measurements of ISRO-GBP", *Current Science*, **120**, 2, 341-351.

Guha, A., De, B. K., Dhar, P., Banik, T., Chakraborty, M., Roy, R., Choudhury, A., Gogoi, M. M., Babu, S. S. and Moorthy, K. K., 2015, "Seasonal characteristics of aerosol black carbon in relation to long range transport over Tripura in Northeast India", *Aerosol and Air Quality Research*, **15**, 3, 786-798.

Guleria, R. P., Kuniyal, J. C. and Dhyani, P. P., 2012a, "Validation of space-born Moderate Resolution Imaging Spectroradiometer remote sensors aerosol products using application of ground-based Multi-wavelength Radiometer", *Advances in Space Research*, **50**, 10, 1391-1404.

Guleria, R. P., Kuniyal, J. C., Rawat, P. S., Thakur, H. K., Sharma, M., Sharma, N. L., Dhyani, P. P. and Singh, M., 2012b, "Validation of MODIS retrieval aerosol optical depth and an investigation of aerosol transport over Mohal in north western Indian Himalaya", *International journal of remote sensing*, **33**, 17, 5379-5401.

Hansen, A., Rosen, H. and Novakov, T., 1984, "The aethalometer-an instrument for the real-time measurement of optical absorption by aerosol particles", *Science of the total environment*, **36**, 191-196.

Hansen, A. and Schnell, R., 2005, "The aethalometer", Magee Scientific Company, Berkeley, California, USA 7.

Jebson, S., 2007, "Fact sheet number 6: the Beaufort Scale".

Jing-Mei, Y., Q. Jin-Huan and Z. Yan-Liang, 2010, "Validation of aerosol optical depth from Terra and Aqua MODIS retrievals over a tropical coastal site in China", *Atmospheric and Oceanic Science Letters*, **3**, 1, 36-39.

Kant, Y., Patel, P., Mishra, A., Dumka, U. and Dadhwal, V., 2012, "Diurnal and seasonal aerosol optical depth and black carbon in the Shiwalik Hills of the north western Himalayas: A case study of the Doon valley, India", *Int. J. Geol. Earth Environ. Sci*., **2**, 2.

Kant, Y., Shaik, D. S., Mitra, D., Chandola, H., Babu, S. S. and Chauhan, P., 2020, "Black carbon aerosol quantification over north-west Himalayas: Seasonal heterogeneity, source apportionment and radiative forcing", *Environmental Pollution*, **257**, 113446.

Kompalli, S. K., Babu, S. S., Udayasoorian, C. and Jayabalakrishnan, R., 2018, "Role of anthropogenic emissions and meteorology on ultrafine particle bursts over a high altitude site in Western Ghats during pre-monsoon", *Journal of Atmospheric and Solar-Terrestrial Physics*, **179**, 378-388.

Kowsalya, M., Sebastian, S. P. and Jayabalakrishnan, R., 2020, "Aerosol Black Carbon Measurement at High Altitude Western Ghats Location of Ooty, Tami Nadu", *International Journal of Environment and Climate Change*, **10**, 12, 390-396.

Krishna Moorthy, K., Babu, S. Suresh, Manoj, M. and Satheesh, S., 2013, "Buildup of aerosols over the Indian Region", *Geophysical research letters*, **40**, 5, 1011-1014.

Krishna Moorthy, K., Babu, S. Suresh and Satheesh, S., 2007, "Temporal heterogeneity in aerosol characteristics and the resulting radiative impact at a tropical coastal station-Part 1: Microphysical and optical properties", *Annales Geophysicae*, **25**, 11, 2293-2308.

Kumar, K. R., Narasimhulu, K., Reddy, R., Gopal, K. R., Reddy, L. S. S., Balakrishnaiah, G., Moorthy, K. K. and Babu, S. S., 2009, "Temporal and spectral characteristics of aerosol optical depths in a semi-arid region of southern India", *Science of the total environment*, **407**, 8, 2673-2688.

Kumar, R., Kumar, G., Kumar, M. and Guleria, R., 2020, "Spectral and Seasonal variations of aerosol optical depth with special reference to Kanpur, Indo-Gangetic Basin", *Indian Journal of Science and Technology*, **13**, 21, 2119-2137.

Kuniyal, J. C., Thakur, A., Thakur, H. K., Sharma, S., Pant, P., Rawat, P. S. and Moorthy, K. K., 2009, "Aerosol optical depths at Mohal-Kullu in the northwestern Indian Himalayan high altitude station during ICARB",, *Journal of Earth System Science*, **118**, 1, 41-48.

Liu, C., Chung, C. E., Yin, Y. and Schnaiter, M., 2018, "The absorption Ångström exponent of black carbon: from numerical aspects", *Atmospheric Chemistry and Physics*, **18**, 9, 6259-6273.

McCartney, E. J., 1976, "Optics of the atmosphere: scattering by molecules and particles", New York.

Moorthy, K., Niranjan, K., Narsimhamurty, B., Agashe, V. and Murthy, B., 1994, "Characteristics of aerosol spectral optical depths over India", *ISRO-IMAP-Scientific Report, SR*, **43**, 1-78.

Moorthy, K. K., Babu, S. S., Sunilkumar, S., Gupta, P. K. and Gera, B., 2004, "Altitude profiles of aerosol BC, derived from aircraft measurements over an inland urban location in India", *Geophysical Research Letters*, **31**, 22.

Moorthy, K. K., Niranjan, K., Narsimhamurty, B., Agashe, V.V.a. and Murthy, B. V. K., 1999, "Aerosol climatology over India", ISRO-GBP; MWR network and database.

Moorthy, K. K., Pillai, P. S. and Babu, S. S., 2003, "Influence of changes in the prevailing synoptic conditions on the response of aerosol characteristics to land-and sea-breeze circulations at a coastal station", *Boundary-layer meteorology*, **108**, 1,145-161.

Moorthy, K. K., Satheesh, S., Babu, S. S. and Dutt, C., 2008, "Integrated campaign for aerosols, gases and radiation budget (ICARB): an overview", *Journal of Earth System Science*, **117**, 1, 243-262.

Moorthy, K. K., Satheesh, S. and Murthy, B. K., 1998, "Characteristics of spectral optical depths and size distributions of aerosols over tropical oceanic regions", *Journal of Atmospheric and Solar-Terrestrial Physics*, **60**, 10, 981-992.

Niranjan, K., Babu, Y. R., Satyanarayana, G. and Thulasiraman, S., 1997, "Aerosol spectral optical depths and typical size distributions at a coastal urban location in India", *Tellus B.*, **49**, 4, 439-446.

Pant, P.a., Hegde, P., Dumka, U., Sagar, R., Satheesh, S., Moorthy, K. K., Saha, A. and Srivastava, M., 2006, "Aerosol characteristics at a high-altitude location in central Himalayas: Optical properties and radiative forcing", *Journal of geophysical research : Atmospheres*, **111,** D17.

Pathak, B., Kalita, G., Bhuyan, K., Bhuyan, P. and Moorthy, K. K., 2010, "Aerosol temporal characteristics and its impact on shortwave radiative forcing at a location in the northeast of India", *Journal of Geophysical Research : Atmospheres*, **115**, D19.

Pavankumari, S., 2015, "Physical and Optical properties of Atmospheric aerosols at Anantapur in Andhra Pradesh", Department of Physics, Sri Krishnadevaraya University.

Prasad, P., Raman, M. R., Ratnam, M. V., Chen, W. N., Rao, S. V. B., Gogoi, M. M., Kompalli, S. K., Kumar, K. S. and Babu, S. S., 2018, "Characterization of atmospheric Black Carbon over a semi-urban site of Southeast India: Local sources and long-range transport", *Atmospheric research*, **213**, 411-421.

Rajesh, T. and Ramachandran, S., 2017, "Characteristics and source apportionment of black carbon aerosols over an urban site", *Environmental Science and Pollution Research*, **24**, 9, 8411-8424.

Raju, M., Safai, P., Sonbawne, S., Buchunde, P., Pandithurai, G. and Dani, K., 2020, "Black carbon aerosols over a high altitude station, Mahabaleshwar: Radiative forcing and source apportionment", *Atmospheric Pollution Research*, **11**, 8, 1408-1417.

Rana, S., Kant, Y. and Dadhwal, V., 2009, "Diurnal and seasonal variation of spectral properties of aerosols over Dehradun, India", *Aerosol and Air Quality Research*, **9**, 1, 32-49.

Ranjan, R. R., Joshi, H. and Iyer, K., 2007, "Spectral variation of total column aerosol optical depth over Rajkot : a tropical semi-arid Indian station", *Aerosol and Air Quality Research*, **7**, 33-45.

Reddy, K. R. O., Balakrishnaiah, G., Gopal, K. R., Reddy, N. S. K., Rao, T. C., Reddy, T. L., Hussain, S. N., Reddy, M. V., Reddy, R. and Boreddy, S., 2016, "Long term (2007-2013) observations of columnar aerosol optical properties and retrieved size distributions over Anantapur, India using Multi Wavelength solar Radiometer", *Atmospheric Environment*, **142**, 238-250.

Remer, L. A., Kaufman, Y., Tanré, D., Mattoo, S., Chu, D., Martins, J. V., Li, R. R., Ichoku, C., Levy, R. and Kleidman, R., 2005, "The MODIS aerosol algorithm, products, and validation", *Journal of atmospheric sciences*, **62**, 4, 947-973.

Resquin, M. D., Santágata, D., Gallardo, L., Gómez, D., Rössler, C. and Dawidowski, L., 2018, "Local and remote black carbon sources in the Metropolitan Area of Buenos Aires", *Atmospheric Environment*, **182**, 105-114.

Rolph, G., Stein, A. and Stunder, B., 2017, "Real-time environmental applications and display system: READY", *Environmental Modelling & Software*, **95**, 210-228.

Safai, P., Raju, M., Rao, P. and Pandithurai, G., 2014, "Characterization of carbonaceous aerosols over the urban tropical location and a new approach to evaluate their climatic importance", *Atmospheric Environment*, **92**, 493-500.

Sagar, R., Kumar, B., Dumka, U., Moorthy, K. K. and Pant, P., 2004, "Characteristics of aerosol spectral optical depths over Manora Peak : A high-altitude station in the central Himalayas", *Journal of geophysical research : Atmospheres*, **109**, D6.

Sandradewi, J., Prévôt, A., Weingartner, E., Schmidhauser, R., Gysel, M. and Baltensperger, U., 2008a, "A study of wood burning and traffic aerosols in an Alpine valley using a multi-wavelength Aethalometer", *Atmospheric Environment*, **42**, 1, 101-112.

Sandradewi, J., Prévôt, A. S., Szidat, S., Perron, N., Alfarra, M. R., Lanz, V. A., Weingartner, E. and Baltensperger, U., 2008b, "Using aerosol light absorption measurements for the quantitative determination of wood burning and traffic emission contributions to particulate matter", *Environmental science & technology*, **42**, 9, 3316-3323.

Schuster, G. L., Dubovik, O. and Holben, B. N., 2006, "Angstrom exponent and bimodal aerosol size distributions", *Journal of Geophysical Research : Atmospheres*, **111**, D7.

Sharma, N. L., Kuniyal, J. C., Singh, M., Dhyani, P. P., Guleria, R. P., Thakur, H. K. and Rawat, P. S., 2012, "Atmospheric aerosol characteristics retrieved using ground based solar extinction studies at Mohal in the Kullu valley of northwestern Himalayan region, India", *Journal of Earth System Science*, **121**, 1, 221-235.

Shaw, G. E., Reagan, J. A. and Herman, B. M., 1973, "Investigations of atmospheric extinction using direct solar radiation measurements made with a multiple wavelength radiometer", *Journal of Applied Meteorology and Climatology*, **12**, 2, 374-380.

Singh, P., Vaishya, A., Rastogi, S. and Babu, S. S., 2020, "Seasonal heterogeneity in aerosol optical properties over the subtropical humid region of northern India", *Journal of Atmospheric and Solar-Terrestrial Physics*" **201**, 105246.

Singh, R. P., Kumar, S. and Singh, A. K., 2018, "Elevated black carbon concentrations and atmospheric pollution around Singrauli coal-fired thermal power plants (India) using ground and satellite data", *International journal of environmental research and public health*, **15**, 11, 2472.

Srivastava, P., Naja, M., Seshadri, T., Joshi, H., Dumka, U., Gogoi, M. M. and Babu, S. S., 2021, "Implications of Site-specific Mass Absorption Cross-section (MAC) to Black Carbon Observations at a High-altitude Site in the Central Himalaya", *Asia-Pacific Journal of Atmospheric Sciences*, 1-14.

Stein, A., Draxler, R. R., Rolph, G. D., Stunder, B. J., Cohen, M. and Ngan, F., 2015, "NOAA's HYSPLIT atmospheric transport and dispersion modeling system", *Bulletin of the American Meteorological Society*, **96**, 12, 2059-2077.

Stocker, T. F., Qin, D., Plattner, G. K., Alexander, L. V., Allen, S. K., Bindoff, N. L., Bréon, F. M., Church, J. A., Cubasch, U. and Emori, S., 2013, "Technical summary", In Climate change 2013: the physical science basis. Contribution of Working Group I to the Fifth Assessment Report of the Intergovernmental Panel on Climate Change, 33-115. Cambridge University Press.

Taneja, K., Attri, S., Ahmad, S., Ahmad, K., Soni, V., Mor, V. and Dhankhar, R., 2017, "Comparative assessment of aerosol optical properties over a mega city and an adjacent urban area in India", *MAUSAM*, **68**, 4, 673-688.

Tiwari, S., Kaskaoutis, D., Soni, V. K., Attri, S. D. and Singh, A. K., 2018, "Aerosol columnar characteristics and their heterogeneous nature over Varanasi, in the central Ganges valley", *Environmental Science and Pollution Research*, **25**, 25, 24726-24745.

Tiwari, S., Pipal, A., Srivastava, A., Bisht, D. and Pandithurai, G., 2015, "Determination of wood burning and fossil fuel contribution of black carbon at Delhi, India using aerosol light absorption technique", *Environmental Science and Pollution Research*, **22** 4, 2846-2855.

Udayasoorian, C., Jayabalakrishnan, R., Suguna, A., Gogoi, M. M. and Babu, S. Suresh, 2014a, "Aerosol black carbon characteristics over a high-altitude Western Ghats location in Southern India", *Annales Geophysicae*, **32**, 10, 1361-1371.

Udayasoorian, C., Jayabalakrishnan, R., Suguna, A., Gogoi, M. M. and Babu, S. Suresh, 2014b, "Aerosol black carbon characteristics over a high-altitude Western Ghats location in Southern India", *Annales Geophysicae.*

Vaishya, A., Singh, P., Rastogi, S. and Babu, S. S., 2017, "Aerosol black carbon quantification in the central Indo-Gangetic Plain: Seasonal heterogeneity and source apportionment", *Atmospheric Research*, **185**, 13-21.

Verma, S., Prakash, D., Srivastava, A. K. and Payra, S., 2017, "Radiative forcing estimation of aerosols at an urban site near the thar desert using ground-based remote sensing measurements", *Aerosol and Air Quality Research*, **17**, 5, 1294-1304.

Weingartner, E., Saathoff, H., Schnaiter, M., Streit, N., Bitnar, B. and Baltensperger, U., 2003, "Absorption of light by soot particles: determination of the absorption coefficient by means of aethalometers", *Journal of Aerosol Science*, **34**, 10, 1445-1463.